Review Article

Xiangping Xu, Xiaodong Wang*, Wang Du, Sudan Liu, Zhongxiang Qiao, and Yabin Zhou

Hydrothermal synthesis of biomass-derived CQDs: Advances and applications

https://doi.org/10.1515/ntrev-2025-0184
received November 6, 2024; accepted May 31, 2025

Abstract: Biomass-based carbon quantum dots (CQDs) are a new type of fluorescent nanomaterial that has received considerable attention due to their low cost, environmental friendliness, and excellent biocompatibility. This review highlights recent progress in the hydrothermal synthesis of these materials, focusing on the use of precursors derived from plants, animals, and microorganisms, as well as their applications in fields such as anti-counterfeiting, wastewater treatment, and biomedical research. Key factors influencing the hydrothermal synthesis, including temperature, pressure, and precursor selection, are discussed. The unique properties and challenges of biomass-derived CQDs are also examined, including issues related to synthesis efficiency, large-scale production, stability, and safety. Future research should aim to optimize synthesis techniques, improve material quality and durability, and address long-term stability and environmental adaptability in practical applications, particularly in anti-counterfeiting technologies. These advancements will further promote the widespread industrial and commercial application of biomass-derived CQDs.

Keywords: carbon quantum dots, biomass, hydrothermal method, green synthesis, anti-counterfeit application

1 Introduction

Carbon quantum dots (CQDs) are carbon-based nanoparticles, primarily composed of carbon, hydrogen, oxygen, and nitrogen. The structure of CQDs is generally considered to consist of two main components: the core, known as the carbon nucleus, primarily composed of sp^2-hybridized carbon atoms, and various functional groups attached to the surface, such as hydroxyl (–OH), carboxyl (–COOH), and amino ($–NH_2$) groups. Carbon dots with hydrophilic groups like hydroxyl and carboxyl on their surface exhibit better water solubility and are classified as water-soluble carbon dots, typically with sizes smaller than 10 nm [1]. As shown in Figure 1, the preparation of CQDs can be categorized into two approaches: top-down and bottom-up. The top-down method utilizes physical and chemical techniques to strip, decompose, or exfoliate bulk carbon materials (such as nanodiamonds, carbon nanotubes, activated carbon, and graphite) into fluorescent nanocarbon particles smaller than 10 nm. Common techniques include arc discharge [2], laser ablation [3], electrochemical methods [4], acid oxidation [5], and ultrasonic treatment [6]. In contrast, the bottom-up approach assembles small carbon precursors, molecules, or oligomers to form nanoscale carbon structures. Compared to the top-down approach, bottom-up methods are more straightforward, cost-effective, and environmentally friendly [7]. Examples of bottom-up techniques include pyrolytic carbonization [8], templating [9], hydrothermal (or solvothermal) [10], microwave-assisted synthesis [11], chemical oxidation [12], stepwise organic synthesis [13], magneto-thermal [14], plasma-induced methods [15], and others.

Biomass is a natural, abundant, and renewable high-carbon resource that includes animals, plants, and microorganisms. Large amounts of waste biomass can contribute to pollution, and most countries opt for incineration to treat this waste. However, due to the high costs involved, only a few countries utilize advanced waste treatment methods, such as pyrolysis [16], carbonization [17], hydrothermal treatment [18], co-firing [19], gasification [20], and biochar [21], to reduce carbon emissions. In recent years, there has been growing interest in the efficient conversion of biomass into low-cost, high-value-added products to help meet the goals of carbon peaking and carbon neutrality while reducing biomass waste pollution [22]. The value of biomass as a precursor for CQDs is increasingly recognized, given its rich heteroatoms, which enable self-doping and result in carbon dots with superior performance [23]. Biomass also

* **Corresponding author: Xiaodong Wang,** School of Police Equipment Technology, China People's Police University, Langfang, Hebei, 065000, China, e-mail: wangxiaodongfy@163.com, tel: +86-15630680031
Xiangping Xu, Wang Du, Zhongxiang Qiao, Yabin Zhou: Graduate School, China People's Police University, Langfang, Hebei, 065000, China
Sudan Liu: School of Immigration Management, China People's Police University, Langfang, Hebei, 065000, China

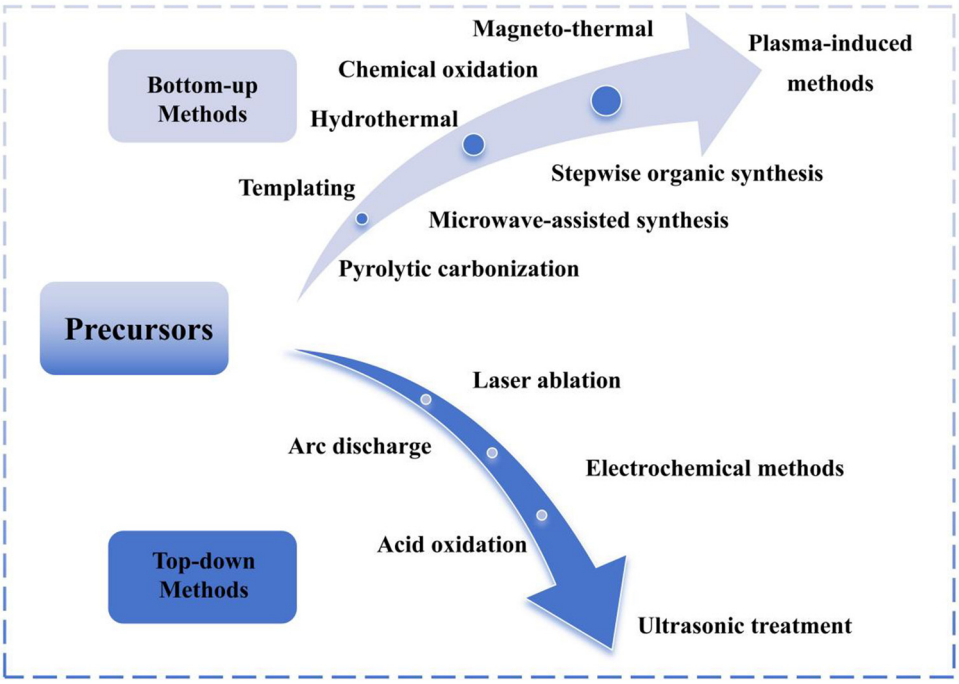

Figure 1: Preparation method of CQDs.

has low toxicity, making it suitable for biological applications, and its low cost makes it ideal for large-scale CQDs production [24]. Thus, converting biomass into CQDs offers significant environmental benefits.

The hydrothermal method has become a primary approach for the synthesis of CQDs due to its mild reaction conditions, simple equipment requirements, and convenient operation [25–27]. This method, particularly in the preparation of CQDs using biomass as a precursor, demonstrates significant comprehensive advantages compared to other methods. These advantages include lower costs, higher environmental friendliness, and better stability, making it widely adopted in practical applications.

A significant advantage of the hydrothermal method is its ability to flexibly control reaction conditions, such as temperature and time, which directly affect the optical properties of CQDs. Wongso *et al.* [28] employed the hydrothermal method to prepare silica-carbon quantum dot (Si-CQDs) composites from rice husk, optimizing the hydrothermal synthesis conditions to enhance the performance of Si-CQDs. The study reveals that the hydrothermal temperature significantly impacts the particle size and optical properties of Si-CQDs. As the temperature increases, the polymerization reaction of the carbon source accelerates, leading to a reduction in particle size. However, excessively high temperatures (above 225°C) can cause over-carbonization, which results in a decrease in fluorescence properties and a transformation of the crystal structure. The pH value during hydrothermal synthesis also plays a critical role. Si-CQDs synthesized under acidic conditions exhibit larger particle sizes and poorer fluorescence performance, whereas alkaline conditions promote the formation of smaller Si-CQDs, significantly enhancing quantum yield (QY) and photoluminescence (PL) intensity. Alkaline environments also reduce surface defects, further improving optical properties. The synergistic effect of temperature and pH is crucial for the final performance of Si-CQDs. By optimally controlling these two parameters, Si-CQDs with excellent optical properties can be obtained, making them suitable for applications such as photocatalysis and sensors. Saafie *et al.* [29] synthesized CQDs from kenaf and found that temperature, precursor mass, and reaction time significantly influenced the synthesis and performance of the CQDs. The variation in temperature played a decisive role in the CQD formation process. At lower temperatures, the reaction rate was slower, resulting in uneven surfaces and imperfect crystal structures, which in turn led to lower QY. At higher temperatures, although the reaction rate increased, excessive temperature could lead to an increase in surface defects and promote particle aggregation, further affecting their fluorescence properties. Therefore, both excessively high and low temperatures were found to be unfavorable for the optical performance of CQDs. Changes in precursor mass also had a significant impact on the quality and performance of CQDs. When the precursor

mass was too low, there was insufficient carbon source, resulting in fewer CQDs with larger particle sizes and poor optical properties. In contrast, an optimal amount of precursor mass provided an adequate carbon source, yielding more uniform CQDs and significantly improving fluorescence performance. However, when the precursor mass was too high, excessive aggregation occurred, which negatively affected the dispersion and optical properties of the CQDs. The reaction time also influenced the properties of CQDs. A shorter reaction time led to incomplete precursor conversion, resulting in larger and aggregated CQDs, which affected their optical properties. Conversely, an excessively long reaction time could cause further aggregation of CQD particles, increasing surface defects and thereby reducing QY.

To provide a more intuitive comparison of the performance differences between the hydrothermal method and other commonly used methods for the preparation of biomass-based CQDs, this study summarizes and compares these methods [30,31], as shown in Table 1. The comparison reveals that the hydrothermal method exhibits significant advantages in terms of cost-effectiveness, stability, and biocompatibility, providing important references for selecting an optimal method for preparing biomass-based CQDs.

In recent years, numerous reviews have been published on the synthesis, chemical, and physical properties of biomass-based CQDs [30,32–36]. However, most of these reviews focus primarily on the application fields of CQDs, with limited systematic discussions on specific synthesis methods. In particular, studies on the hydrothermal synthesis of biomass-based CQDs lack comprehensive summaries and in-depth analyses. Therefore, a systematic review in this area is of significant importance.

The primary innovation of this review lies in its comprehensive exploration of anti-counterfeiting applications. Unlike existing reviews, this work is the first to systematically consolidate research findings on biomass-derived CQDs specifically in the field of anti-counterfeiting. By presenting detailed tables, the review provides a clear and concise summary of the current state and key features of anti-counterfeiting applications, making it both structured and reader-friendly. Additionally, this article offers novel insights into the limitations and future prospects of anti-counterfeiting applications, serving as a valuable reference for advancing research in this domain. These contributions not only address gaps in the existing literature but also underscore the potential and advantages of hydrothermally synthesized biomass-based CQDs in anti-counterfeiting technologies. Furthermore, the review adopts a similar tabular approach to summarize research progress in other application areas, offering readers a more comprehensive understanding of the diverse applications of biomass-derived CQDs.

2 Different types of biomass-based CQD carbon sources

During the hydrothermal synthesis of CQDs, the choice of carbon source plays a critical role. Different types of biomass not only determine the fluorescent properties and structural characteristics of CQDs but also significantly influence their suitability for practical applications. As shown in Figure 2, carbon sources can be broadly categorized into three main types: plant-based, animal-based, and microbial-based. These categories are further subdivided into plant waste, edible plant materials, animal-derived materials, and microbial materials. Figure 2 visually illustrates the diversity of biomass-derived carbon sources, offering a wide range of options for hydrothermal CQDs synthesis and highlighting the potential of different carbon sources in performance tuning.

This section further explores the applications and characteristics of plant-, animal-, and microorganism-

Table 1: Comparison of common methods for preparing CQDs from biomass precursors

	Hydrothermal (bottom up)	Pyrolysis (bottom up)	Microwave (bottom up)	Ultrasonic (top down)	Acid oxidation (top down)
Economic feasibility	Low cost	Moderate cost	Moderate cost	Low cost	Moderate cost
Environmental friendliness	High	High	General	High	Low
Stability	High	High	High	High	General
Reusability	Good	Moderate	General	General	General
Cytotoxicity	Low	Low	Low	Low	High
Biocompatibility	Good	Moderate	Good	Good	Poor
Particle size control	Poor	Moderate	Poor	Poor	Moderate

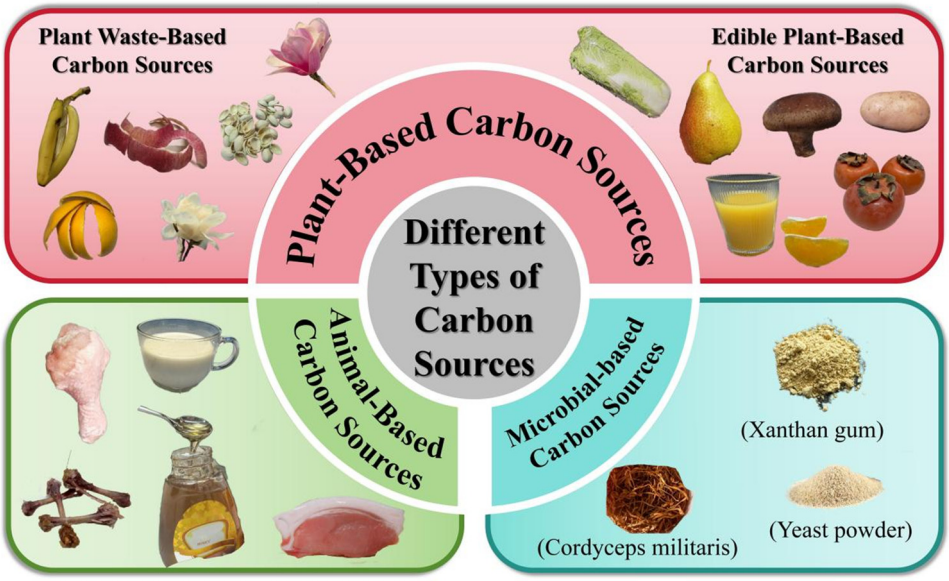

Figure 2: Biomass CQDs from different types of carbon sources.

based biomass in the hydrothermal synthesis of CQDs. By classifying and analyzing these various carbon sources, we aim to provide a clearer understanding of the advantages and suitability of each type of biomass for hydrothermal synthesis. This analysis serves as a reference for optimizing CQD synthesis processes and tailoring their properties for specific applications.

2.1 Plant-based carbon sources

Plant-based carbon sources have garnered significant attention in biomass-based CQDs research due to their wide availability, low cost, and renewability. These carbon sources not only allow for the effective utilization of agricultural and industrial waste, reducing environmental impact, but can also be extracted from edible plants. Based on their sources and applications, plant-based carbon sources can be further divided into plant waste-based carbon sources and edible plant-based carbon sources.

2.1.1 Plant waste-based carbon sources

Plant waste offers significant advantages as a carbon source due to its wide availability, low cost, and environmental friendliness. It is typically rich in lignin, cellulose, and other rigid, hard-to-degrade components, which not only serve as abundant carbon sources but also impart unique electronic properties during the hydrothermal synthesis of CQDs. In particular, lignin and lignin-like structures, under appropriate degradation conditions, can promote electron conjugation, thereby enhancing the photostability of CQDs. The common feature of plant waste is its richness in complex organic substances (such as lignin and cellulose), which facilitate CQD synthesis but may also influence their optical properties. By optimizing reaction conditions and refining the hydrothermal synthesis process, the QY of waste-derived CQDs can be effectively improved, while leveraging their unique structural characteristics to enhance photostability and expand their application potential. Table 2 summarizes the current status of research on the hydrothermal synthesis of CQDs from plant waste-based carbon sources.

Atchudan *et al.* [37,38] synthesized CQDs with high QYs of 23 and 20%, respectively, using dwarf banana peels and common banana peels as carbon sources *via* the hydrothermal method. Figure 3(a) illustrates the detailed synthesis process of luminescent nitrogen-doped CQDs derived from dwarf banana peels, demonstrating that during hydrothermal treatment, the organic molecules and elements in the peels decompose under high temperature and pressure, forming CQDs with luminescent properties. Figure 3(b) presents the plausible formation mechanism of CQDs synthesized from common banana peels, highlighting the decomposition of organic molecules in the peels, which contributes to the high QY of the resulting CQDs. These illustrations clearly reveal the influence of different banana peel sources on CQD synthesis and underscore the critical role of the hydrothermal method in the

Table 2: Hydrothermal synthesis of CQDs from plant waste-based carbon sources

Carbon source	Synthetic conditions	Size (nm)	QY (%)	Ref.
Kenaf	200°C, 24 h	—	76.12	[29]
Dwarf banana peel	200°C, 24 h	2.5–5.5	23	[37]
Banana peel	200°C, 24 h	3.6	20	[38]
Citrus limetta peel	185°C, 24 h	3	—	[39]
Pomelo peel	200°C, 3 h	2–4	6.9	[40]
Orange peel	180°C, 3 h	3.5–5.5	35.37	[41]
Avocado peel	180°C, 24 h	2.22	—	[42]
Palm kernel shell	160°C, –	4.5	2.4	[43]
Phytic acid	200°C, 4 h	4.03	22	[44]
Eucalyptus leaf (*Eucalyptus globulus*)	180°C, 24 h	6.33	60.7	[45]
Willow leaf	200°C, 12 h	—	—	[46]
Psidium guajava L. (Guava) leaf	180°C, 5 h	2.9	9.2	[47]
Mango leaf	200°C, 35 min	5–10	16	[48]
Prosopis juliflora leaf	180°C, 5 h	8	7.88	[48]
Apple peel	200°C, 18 h	1.96	9.43	[49]
Lychee shell	180°C, 9 h	—	7.86	[50]
Rice residue	200°C, 12 h	2.7	23.48	[51]
Wheat straw	250°C, 10 h	1.7	9.2	[52]
Corn cob powder	180°C, 12 h	2.54	1.05	[53]
Wolfberry straw	200°C, 24 h	1.7–2.5	59	[54]
Starch fermentation wastewater	180°C, 10 h	4.2	24.5	[55]
Cigarette smoke	180°C, 2 h	6.3	—	[56]
Banana petiole	200°C, 5 h	3.27	8.53	[57]
Poplar wood powder	200°C, 6 h	5–10	—	[58]
Salix wood powder	180°C, 12 h	2.19	—	[59]
Pistachio shells	200°C, 1 h	4	15	[60]
Magnolia flower	200°C, 12 h	Purple flower: 3.9 White flowers: 10.1	Purple flower: 11.9 White flowers: 10.4	[61]
Parthenium hysterophorus leaf	140°C, 1 h	4.4	10.2	[62]
Rhizome of Acorus calamus	200°C, 6 h	6	15	[63]
Laurel leaf	180°C, 5 h	3.8	49.9	[64]
Kiwi fruit (*Actinidia Deliciosa*) peel	200°C, 24 h	5	18	[65]
Wasted coffee ground	220°C, 20 h	2.18	—	[66]
Poplar aspen wood powder	200°C, 6 h	3.4–4.6	47.4	[67]
Cherry blossom flowers	200°C, 20 h	4.86	—	[68]
Alkali-soluble xylan	200°C, 12 h	6.92	16.18	[69]
Xylose	180°C, 4 h	3.5–4	6.2	[70]
Cellulose	300°C, 24 h	3.8	10.9	[71]
Oxidized cellulose	200°C, 10 h	1.86	30.3	[72]
Pre-hydrolyzed lignin	220°C, 11 h	5.91	13.5	[73]
Corncob lignin	240°C, 10 h	7.83	46.38	[74]
Alkali lignin	200°C, 12 h	5.05	30.5	[75]

synthesis process. Han *et al.* [41] achieved a QY of 35.37% using orange peel as a carbon source, completing the synthesis in just 3 h, making it highly efficient and promising. Xing *et al.* [44] used phytic acid to produce CQDs with a QY of 22%. The high QY is attributed to the multifunctional groups and doping effects of phytic acid. Phytic acid molecules contain abundant phosphate and hydroxyl groups, which participate in CQDs formation during hydrothermal synthesis and create a wealth of surface functional groups. Phosphorus from phytic acid can be doped into the CQDs structure to form phosphorus-doped carbon quantum dots (P-CQDs), significantly enhancing their optical properties and QY. Johny *et al.* [45] synthesized CQDs from eucalyptus leaves, achieving an ultra-high QY of 60.7%. This was attributed to the high carbohydrate, cellulose, and lignin content in eucalyptus leaves, which are also rich in hydrocarbon groups and organic compounds like phenols and alcohols – functional groups that facilitated surface functionalization of the CQDs during synthesis [76]. Xu *et al.* [54] optimized reaction

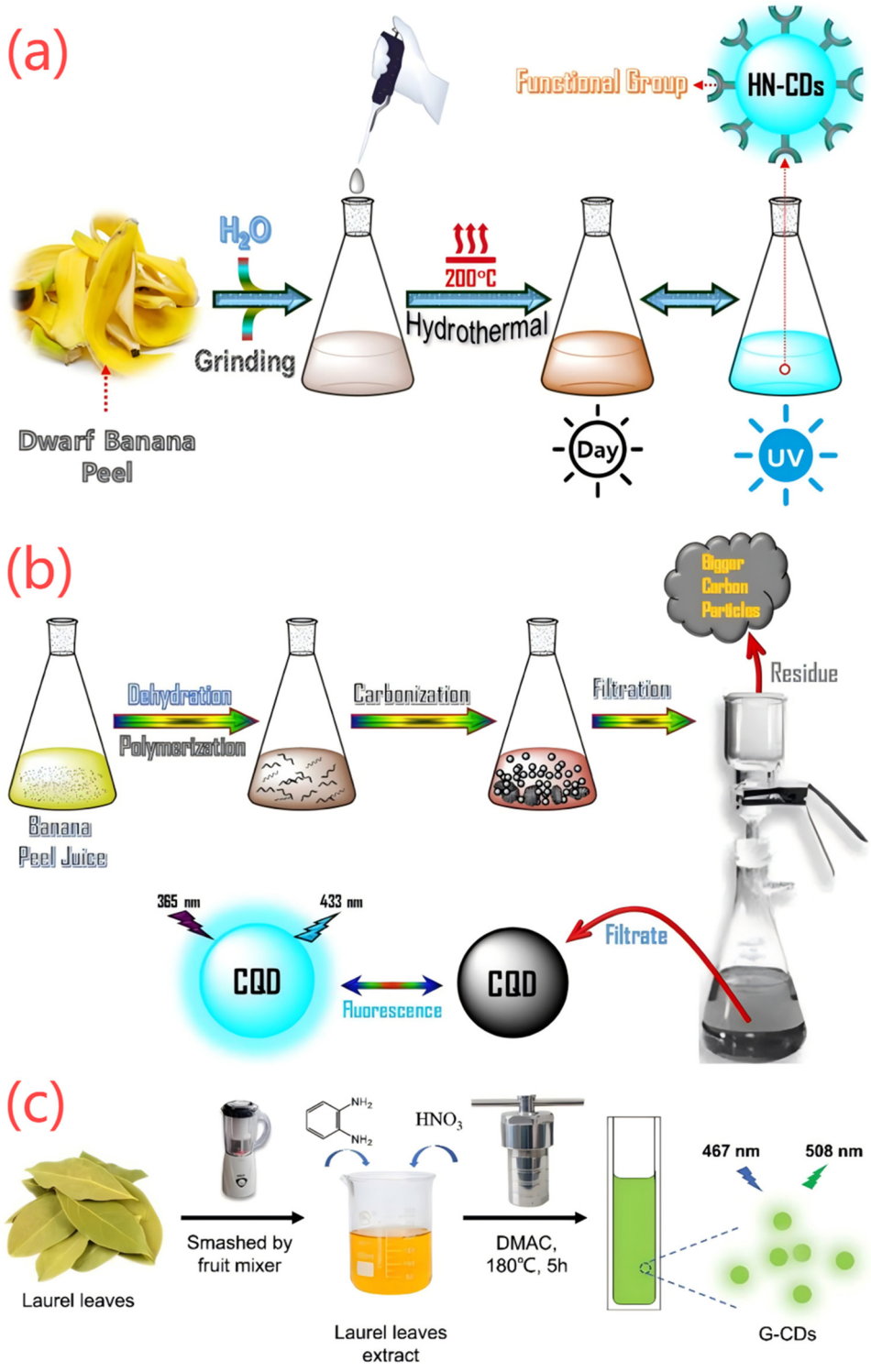

Figure 3: (a) Illustration of the synthesis procedure of fluorescent HN-CDs from dwarf banana peel. Reprinted from Atchudan *et al.* [37], copyright (2020), with permission from Elsevier. (b) Plausible formation mechanism of CQDs from the banana peel by hydrothermal process. Reprinted from Atchudan *et al.* [38], copyright (2021), with permission from Elsevier. (c) Schematic diagram of CQDs synthesized using Laurel leaves as a carbon source. Reprinted from Long *et al.* [64], Copyright (2023), with permission from Elsevier.

conditions, including reaction time, temperature, and wolfberry straw concentration (7.5 g/L), to achieve a QY of 59% by heating at 200°C for 24 h. Man *et al.* [55] prepared CQDs with a QY of 24.5% using starch fermentation wastewater, demonstrating not only the reuse of waste materials but also a reduction in environmental pollution. During the synthesis, residual amino acids and other organic compounds in the wastewater formed reactive groups like –COOH and –C═O on the CQDs surface, enhancing their fluorescence properties. Long *et al.* [64] synthesized green carbon quantum dots (G-CDs) with a remarkable QY of 49.9% using laurel leaves as the carbon source, *o*-phenylenediamine (OPD) as the nitrogen source, and *N*,*N*-dimethylacetamide (DMAC) as the solvent through a one-step hydrothermal method. Figure 3(c) illustrates the synthesis process of these green CQDs: laurel leaves, OPD, and DMAC were mixed and reacted under hydrothermal conditions. Structural characterization revealed the presence of abundant nitrogen-containing functional groups on the surface of the CQDs, which played a crucial role in enhancing their PL properties, significantly improving both QY and fluorescence intensity. This study provides a novel approach for the synthesis of green CQDs and highlights the impact of different raw materials and reaction conditions on CQD performance. Gong *et al.* [67] synthesized water-soluble CQDs with a QY of 47.4% from poplar wood powder, and found that these CQDs were rich in –OH, NH_3, and –COOH functional groups. Liu *et al.* [72] found that the chemical accessibility and reactivity of cellulose were significantly improved after oxidation treatment. Cellulose also provides additional functional groups, contributing to improved CQD QYs. Yang *et al.* [73] synthesized sulfur-doped carbon quantum dots (SCQDs) using hydrolyzed lignin as a carbon source. These SCQDs exhibited excellent fluorescence stability in acidic environments, with a QY of 13.5%. The sulfur doping introduced numerous sulfur atoms on the surface of the CQDs, forming new surface states that promoted radiative recombination, thereby increasing the QY. Yang *et al.* [74] used corn kernel lignin as a carbon source and applied a co-doping technique with magnesium and nitrogen, which significantly increased the CQD QY to 46.38%. This dual doping improved CQD optical properties and broadened their emission spectrum, making them suitable for various optical applications. Zhu *et al.* [75] synthesized CQDs with a QY of 30.5% using alkali lignin as the carbon source. The high yield was attributed to the aromatic ring structures in alkali lignin, which contains numerous aromatic rings and oxidized branched chains rich in unsaturated bonds (*e.g.*, C═C and C═O), making it an ideal carbon source for CQDs synthesis.

2.1.2 Edible plant-based carbon sources

The chemical composition and structural characteristics of edible plants have a significant impact on the QY of CQDs. Edible plants rich in nitrogen- or oxygen-containing functional groups provide more active sites, which contribute to enhanced optical properties. Additionally, plants with abundant aromatic rings and flavonoids improve the conjugation of electrons, thereby optimizing the light absorption and emission properties of CQDs. Therefore, selecting suitable edible plant materials and optimizing their chemical composition and structural features can effectively regulate the optical performance of CQDs. Table 3 summarizes the current research on hydrothermal synthesis of CQDs from edible plant-based carbon sources.

Miao *et al.* [80] synthesized CQDs with a QY of 27.9% using tobacco as the carbon source, attributing the high yield to the one-pot hydrothermal synthesis. The abundant carbon content and surface oxygen-containing functional groups, such as carbonyl and hydroxyl, provided stability and favorable optical properties during CQDs formation. Pakchoi (*Brassica rapa* subsp. *chinensis*), commonly known as baby bok choy, is a leafy vegetable whose chlorophyll and organic molecules serve as rich precursors for CQDs formation. Cui *et al.* [82] used pakchoi to prepare CQDs with a QY of 10.28%, enhanced by combining solvent extraction and solvothermal methods, which resulted in a significant single-excitation dual-emission property. Xie *et al.* [83] synthesized CQDs using highland barley as a carbon source, achieving a high QY of 14.4%. Figure 4(a) illustrates the synthesis process of these green CQDs, where highland barley was pyrolyzed under hydrothermal conditions at elevated temperatures, resulting in the successful production of CQDs with high QY. The carbohydrates and proteins abundant in highland barley were transformed into efficient fluorescence emission centers during the pyrolysis process, significantly enhancing the PL properties of the CQDs. Xu *et al.* [84] demonstrated excellent fluorescence properties and high QY of CQDs synthesized from Maofeng tea leaves. Figure 4(b) illustrates the formation process of CQDs derived from tea leaves, where hydrothermal treatment successfully converted the natural components of tea leaves into high-yield CQDs. The polyphenols and other organic compounds abundant in tea leaves were transformed into efficient luminescent centers during the thermal process, significantly enhancing the PL properties of the CQDs. These efficient luminescent centers endow the material with broad potential for multifunctional applications, particularly in bioimaging and sensing. Li *et al.* [86] synthesized CQDs with a QY of 31.7% from orange juice and

Table 3: Hydrothermal synthesis of CQDs from edible plant-based carbon sources

Carbon source	Synthetic conditions	Size (nm)	QY (%)	Ref.
Lentinus polychrous Lèv	200°C, 12 h	6	6.4	[77]
Northern Shaanxi potatoes	200°C, 12 h	5	16.96	[78]
Traditional Chinese medicine *Codonopsis pilosula*	180°C, 3 h	1.6–4.6	—	[79]
Tobacco	200°C, 3 h	2.14	27.9	[80]
Honeysuckle	200°C, 9 h	1.76	—	[81]
Pakchoi (*Brassica rapa* subsp. *chinensis*)	200°C, 10 h	3	10.28	[82]
Highland barley	200°C, 24 h	5.8	14.4	[83]
Maojian (a kind of famous green teas)	200°C, 3 h	13	12.79	[84]
Rambutan seed	200°C, 20 h	3.07	16.97	[85]
Orange juice	200°C, 11 h	1.86	31.7	[86]
Phyllanthus acidus (*P. acidus*)	180°C, 8 h	4.5	14	[87]
Lime (*Citrus aurantifolia*)	180°C, 6 h	—	—	[88]
The unripe fruit of Prunus persica (peach)	180°C, 5 h	8	15	[89]
Papaya	200°C, 5 h	2–6	18.98	[90]
Pyrus pyrifolia (pear) fruit	180°C, 6 h	2	10.8	[91]
Lycium ruthenicum	180°C, 9 h	4.05	10.63	[92]
Chionanthus retusus (*C. retusus*) fruit	180°C, 6 h	5	9	[93]
Seville orange (*Citrus aurantium*)	130°C, 12 h	4.8	13.3	[94]
Ganoderma lucidum	180°C, 6 h	4.09	6.26	[95]
Tylophora indica plant	180°C, 10 h	4.3	16.1	[96]
Mopan persimmons	150°C, 4 h	3.18	8.39	[97]
Chinese herbal residues	200°C, 8 h	2.8	4	[98]
Zanthoxylum bungeanum	180°C, 5 h	B-CDs: 3.5 G-CDs: 4 R-CDs: 7.5	B-CDs: 13.1 G-CDs: 11.2 R-CDs: 9.8	[99]
Aloe carazo leaf	200°C, 12 h	5.64	21.4	[100]
Tapioca starch	175°C, 1 h	9.54	1.167	[101]
Pine pollen	200°C, 20 h	3.77	—	[102]
Citron fruit	180°C, 7 h	4	34.5	[103]
Chlorogenic acid	230°C, 2 h	2–5	—	[104]
Ginsenoside Rb1	200°C, 24 h	7.14	—	[105]
Quinoa saponin	200°C, 10 h	2.25	22.24	[106]
Proanthocyanidin	200°C, 10 h	9.78	—	[107]
Folic acid	200°C, 5 h	6.8	41.8	[108]
Zucchini	180°C, 6 h	2.5~3.5	12.19	[109]

ethylenediamine, largely due to the abundant surface defects and functional groups. Nitrogen doping effectively disrupted the large conjugated carbon structure, enhancing fluorescence performance. *Phyllanthus acidus* (*P. acidus*), a natural material rich in organic acids and antioxidants, is an environmentally friendly and easily accessible carbon source. The polyphenolic compounds in *P. acidus* aid in the synthesis of CQDs with a QY of 14% [87]. Liao *et al.* [99] reported a method for synthesizing multicolor fluorescent CQDs using *Zanthoxylum bungeanum* (Sichuan pepper) as the carbon source. Figure 4(c) illustrates the synthesis process of these multicolor fluorescent CQDs. By varying the nitrogen source, the researchers utilized a hydrothermal method to produce blue, green, and red fluorescent carbon dots (B-CDs, G-CDs, and R-CDs) with stable optical properties and high QYs. The emission wavelengths of these CQDs were 492, 523, and 601 nm, with corresponding QYs of 13.1, 11.2, and 9.8%, respectively. Furthermore, the CQDs demonstrated excellent salt tolerance, photobleaching resistance, and chemical stability, highlighting their broad potential for applications, particularly in the field of anti-counterfeiting fluorescent inks. These properties make them ideal materials for anti-counterfeiting technologies, capable of maintaining stable luminescence under various environmental conditions. Serag *et al.* [108] synthesized CQDs with a high QY of 41.8% using folic acid as the carbon source. The high QY is due to folic acid's ability to form CQDs with high crystallinity and uniform particle size under high temperature and pressure in hydrothermal conditions. High crystallinity leads to fewer defects and a more regular lattice structure, reducing nonradiative recombination and energy loss, thereby

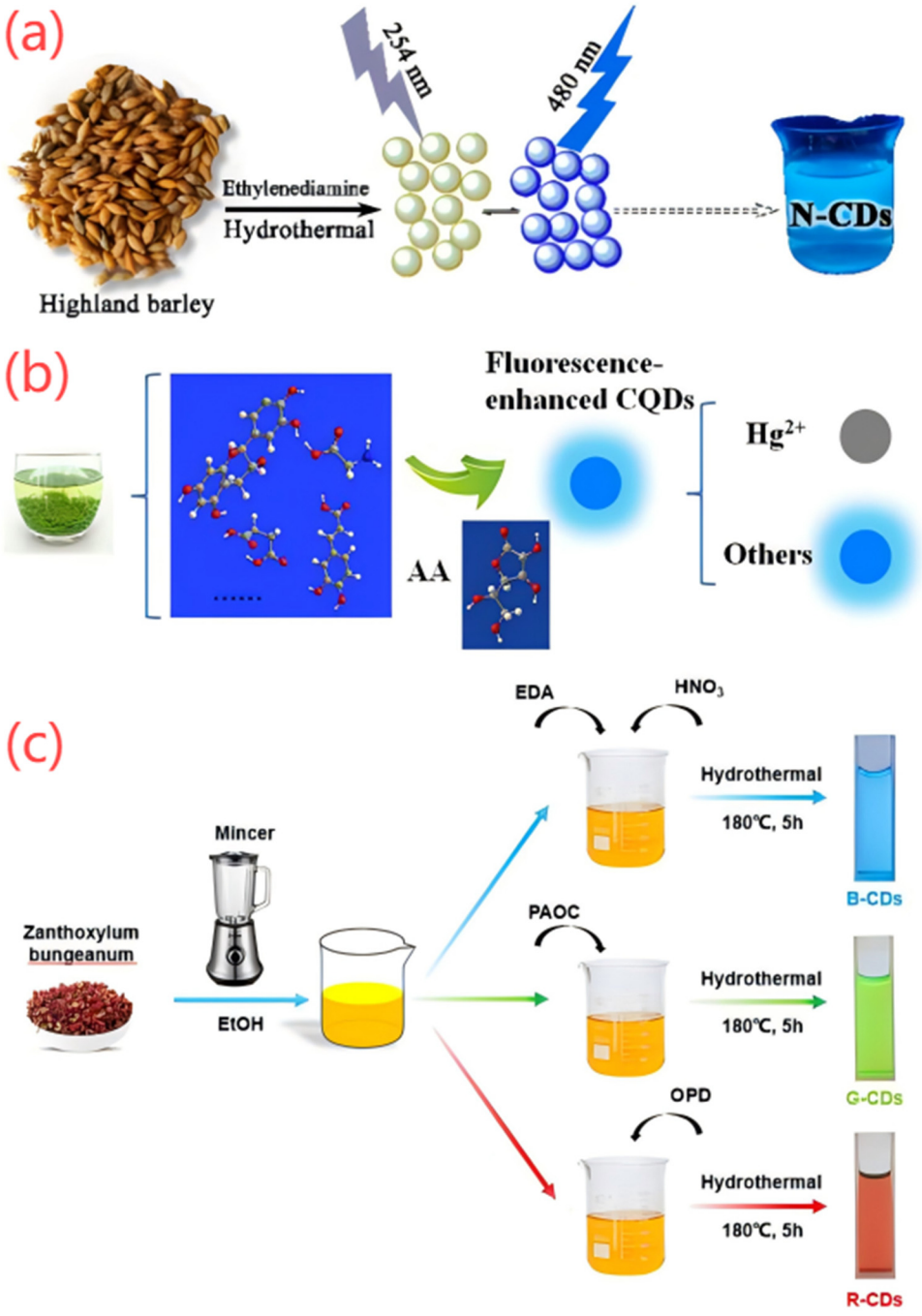

Figure 4: (a) The preparation process of the N-CDs by the hydrothermal method from Highland barley. Reprinted from Xie *et al.* [83], open access under the Creative Commons license. (b) Illustration of the formation process of (AA)-enhanced CQDs from green teas by hydrothermal treatment and their multi-function application. Reprinted from Xu *et al.* [84], copyright (2019), with permission from Elsevier. (c) Synthesis of multicolor fluorescent CDs from *Zanthoxylum bungeanum* as the carbon source *via* the hydrothermal method. Reprinted from Liao *et al.* [99], copyright (2023), with permission from Elsevier.

improving fluorescence performance and QY. Folic acid also contains abundant nitrogen, which can be doped into CQDs during synthesis, further enhancing fluorescence properties and QY.

2.2 Animal-based carbon sources

The choice of carbon source is critical to the optical properties and application potential of CQDs. Animal-based

carbon sources differ significantly from plant-based carbon sources in terms of chemical composition and structure. Unlike plant-based carbon sources, animal-derived materials primarily consist of proteins, amino acids, and chitin. These components not only provide nitrogen sources but also react with other components of the carbon source, influencing the surface functional groups and optical properties of CQDs, thereby enhancing their QY and photostability. Compared to plant-based sources, animal-based carbon sources can impart strong nitrogen-doping characteristics to the surface of CQDs due to their rich nitrogen content, which contributes to improved optical performance. Additionally, animal-based carbon sources often exhibit strong surface functionalization capabilities, making them more promising for applications in sensing and catalysis.

The variations in chemical composition and structure among different animal-based carbon sources also result in differences in CQDs' performance. Generally, animal-derived materials lack the complex cellulose and lignin structures found in plant-based sources. However, their high protein and amino acid content, along with certain specific macromolecules such as chitin and their ability to bind metal ions, allow CQDs synthesized from these sources to exhibit unique advantages in photostability, functionalization, and metal doping.

In summary, animal-based carbon sources possess distinct advantages in nitrogen doping, surface functionalization, and metal ion doping, which significantly influence the optical properties and application potential of CQDs. When selecting an appropriate carbon source, it is essential to consider the impact of its chemical composition and structural characteristics on CQDs' performance. Table 4 summarizes the current research on hydrothermal synthesis of CQDs from animal carbon sources.

Table 4: Hydrothermal synthesis of CQDs from animal carbon sources

Carbon source	Synthetic conditions	Size (nm)	QY (%)	Ref.
Oyster shell	160°C, –	6	1.4	[43]
Fish scale of the crucian carp	200°C, 20 h	5–10	6.9	[110]
Poultry chicken feather	200°C, 7 h	—	57	[111]
Crayfish shell	180°C, 8 h	3.8	10.68	[112]
Horse spleen ferritin	200°C, 12 h	2–4	5.81–10.61	[113]
Chitosan	200°C, 10 h	2.13	38	[114]
Pigeon manure	150°C, 6 h	15.65	25.92	[115]
Wool keratin	200°C, 10 h	2–6	8	[116]
Cow milk	180°C, 2 h	7	38	[117]
Cow milk	180°C, 12 h	1–5	18	[118]
Chicken bone	180°C, 4 h	3.2	—	[119]
Mussel	150°C, 8 h	1.3	15.2	[120]
Crab shell	180°C, 12 h	10	—	[121]
Chicken cartilage	200°C, 8 h	7.6	10.3	[122]
Fingernail	200°C, 3 h	3.1	—	[123]
Chicken drumstick	190°C, 5 h	5	32.86	[124]
Pork liver	180°C, 5 h	3.2	11.74	[125]
Natural honey	200°C, 6 h	8.29	4.19	[126]
Silk fibroin	220°C, 6 h	7.5	38	[127]
Spider silk	180°C, 10 h	3.65	21.5	[128]
Pork skin collagen	240°C, 3 h	1.25	15	[129]
Fish scales	200°C, 20 h	4–9	9	[130]
Pork	200°C, 10 h	3.5	17.3	[131]
Bombyx mori silk	200°C, 3.5 h	5.6	61.1	[132]
Wool and pig hair	240°C, 6 h	5.9	25.6	[133]
Pigskin	250°C, 2 h	5.58	24.1	[134]
Prawn shell	180°C, 12 h	3	—	[135]
Cocoon silk	260°C, 50 min	7.4	24	[136]

Chen *et al.* [112] synthesized CQDs from crayfish shells with a QY of 10.68%. Crayfish shells, rich in chitin and protein, are ideal precursors for nitrogen-rich carbon dots. The preparation process is inexpensive and simple, and it effectively utilizes large amounts of crustacean waste, reducing environmental pollution. Hastuti *et al.* [111] used chicken feathers as a carbon source to synthesize CQDs, achieving an ultra-high QY of 57%. They found that the hydrothermal time and temperature significantly influenced the yield, with the highest yield of 57% obtained after 7 h of reaction at 200°C. Additionally, functional groups formed during hydrothermal treatment, such as C═C, O–H, C–N, C–H, C═O, and C–O–C, and their transformations positively impacted the optical properties of the CQDs. Shen *et al.* [113] synthesized metal-doped CQDs using horse spleen ferritin as a carbon source, doping the CQDs with Co^{2+}, Fe^{2+}, Cu^{2+}, Mg^{2+}, Mn^{2+}, Ni^{2+}, Zn^{2+}, and Gd^{2+}. The QYs of the nine resulting samples (including a blank control) ranged from 5.81 to 10.61%, with the Zn-doped CQDs exhibiting the highest QY, indicating that metal-doped CQDs from ferritin possess good optical properties. Narimani and Samadi [124] synthesized novel CQDs using chicken drumsticks as a carbon source *via* a green, low-cost hydrothermal method without the use of surface passivating agents or chemical reagents. The resulting CQDs exhibited blue fluorescence emission, a high QY of approximately 32.86%, and excellent water solubility. Liu *et al.* [132] synthesized CQDs from Bombyx mori silk with a QY of 61.1%. These nitrogen-doped CQDs exhibited excellent optical properties and stability, maintaining photostability under strong acids or bases, high salt concentrations, and most organic solvents.

- Interestingly, although both studies used cow milk as a carbon source to synthesize CQDs, differences in

synthesis conditions and post-processing steps led to significant variations in QY and size. Kumar *et al.* [117] used a simple hydrothermal method to carbonize milk components under high temperature and pressure, producing CQDs with an average size of approximately 7 nm and a QY of 38%. In contrast, Han *et al.* [118] incorporated an additional ethyl acetate extraction step and ultraviolet (UV) irradiation to form complexes with silver nanoparticles, yielding smaller CQDs (1–5 nm). However, the more complex purification and functionalization processes led to a reduction in QY. The two studies also differed in their approach to surface functionalization. The CQDs synthesized by Kumar *et al.* had stabilized surface functional groups, making them suitable for sensing applications. In contrast, Han *et al.* introduced amphiphilic functional groups, resulting in silver nano-complexes with antimicrobial properties. Thus, although both studies used the same carbon source, the variations in synthesis and treatment significantly impacted the physicochemical properties and potential applications of the CQDs.

2.3 Microbial-based carbon source

Unlike plant-based and animal-based carbon sources, microbial-based carbon sources, such as yeast powder and yeast cell walls, offer abundant carbon resources due to their complex cell wall structures, which are rich in polysaccharides, proteins, and lipids. Microbial-based carbon sources not only exhibit high biocompatibility but also allow for the optimization of the optical properties of CQDs by adjusting reaction conditions. During the synthesis of CQDs, the polysaccharides and proteins in microbial carbon sources provide ample carbon content, while the lipid components contribute to improved hydrophobicity and surface activity. Moreover, the diversity and complexity of microbial carbon sources enable multiple possibilities for surface modification and the introduction of functional groups in CQDs. Table 5 summarizes the current research on the hydrothermal synthesis of CQDs using microbial-based carbon sources.

Mirseyed *et al.* [137] demonstrated that yeast cell walls can be used as a carbon source to synthesize CQDs with a QY of 19%. Figure 5 illustrates the composition and structure of yeast cell walls, which consist of inner and outer layers. The inner layer is primarily composed of chitin and β-1,3- and β-1,6-glucans, while the outer layer is made up of mannoproteins and glycoproteins. Yeast cell walls are rich in carbon sources, such as glucans and mannoproteins,

Table 5: Hydrothermal synthesis of CQDs by microbial-based carbon sources

Carbon source	Synthetic conditions	Size (nm)	QY (%)	Ref.
Yeast powder	180°C, 5 h	2.98	9.8	[81]
Cell walls from *Saccharomyces cerevisiae*	250°C, 5 h	3.2	19	[137]
Spirulina	150°C, 6 h	1.83	3.72	[138]
Cordyceps militaris	180°C, 6 h	—	12.9	[139]
Xanthan gum	180°C, 6 h	2.6	7.7	[140]
Oxidized xanthan gum		2.4	2.7	
Exopolysaccharide	200°C, 12 h	20	—	[141]

which are transformed into the core structure of CQDs during the hydrothermal carbonization process. Additionally, yeast cell walls contain heteroatoms such as phosphorus, nitrogen, and sulfur, which are naturally doped into the CQDs during synthesis. This doping not only modulates the electronic structure of CQDs but also significantly enhances their fluorescence intensity and QY. Furthermore, heteroatom doping optimizes the optical properties of CQDs, improving their biocompatibility and multifunctionality. The surface of yeast cell walls is also enriched with functional groups, including hydroxyl, carboxyl, and amino groups, which play a passivating role on the surface of CQDs. These functional groups reduce surface defects, thereby enhancing the optical properties and chemical stability of CQDs. Overall, yeast cell walls exhibit strong potential as an efficient carbon source for the synthesis of CQDs and show promising applications in fields such as bioimaging and sensing. Kalpana *et al.* [141] selected exopolysaccharides as the carbon source for synthesizing CQDs due to their unique advantages. Exopolysaccharides, naturally occurring high-molecular-weight polymers produced by bacteria, are rich in various functional groups such as hydroxyl, carboxyl, and amino groups. These functional groups provide excellent surface modification during the synthesis process, reducing surface defects and enhancing both optical performance and chemical stability of the CQDs. Additionally, exopolysaccharides contain abundant elements like carbon, nitrogen, and oxygen, which can effectively be converted into the core structure of CQDs during hydrothermal carbonization. The nitrogen content, in particular, helps modulate the electronic structure of the CQDs, further improving their fluorescence intensity and QY. More importantly, the biocompatibility and environmental friendliness of exopolysaccharides make them an ideal carbon source for synthesizing high-performance CQDs. These unique properties not only enhance the fluorescence performance

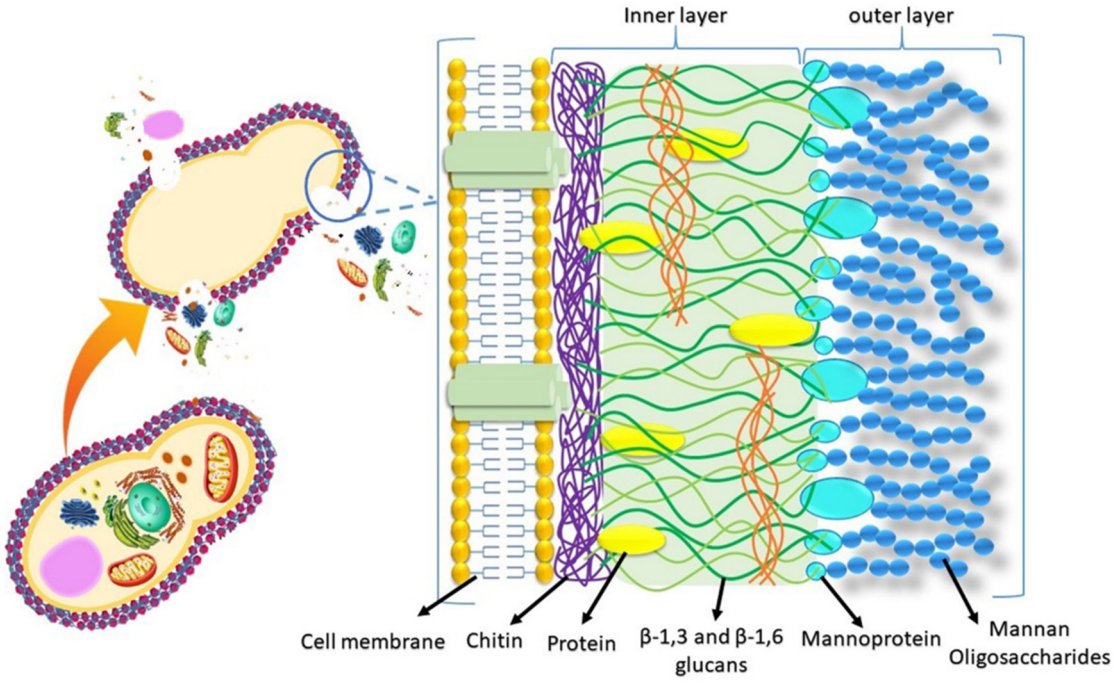

Figure 5: Schematic illustration of the Saccharomyces cerevisiae's cell wall and the components of its two layers. Reprinted from Mirseyed *et al.* [137], open access under the Creative Commons license.

of CQDs but also bolster their potential applications in fields such as biomedicine and environmental protection. Therefore, using exopolysaccharides as a carbon source for CQDs synthesis offers significant advantages, promoting the efficient synthesis of CQDs and optimizing their optical and biological properties.

3 Progress in the application of hydrothermal synthesis of biomass-based CQDs

3.1 Anti-counterfeiting

Biomass-based CQDs show significant potential for anti-counterfeiting applications, primarily due to their excellent fluorescence properties and stability [142]. CQDs synthesized *via* the hydrothermal method are simple and cost-effective to produce, and their use in anti-counterfeiting heavily depends on their solid-state fluorescence. However, particle aggregation often leads to a phenomenon known as aggregation-caused quenching (ACQ), where fluorescence is significantly reduced in the solid state compared to in solution [143]. One effective way to mitigate this quenching is by dispersing CQDs in a polymer matrix [144]. Poly (vinyl alcohol) (PVA) is commonly considered a suitable matrix due to its excellent surface passivation ability and strong compatibility with CQDs [145]. Additionally, other materials such as carboxymethyl cellulose (CMC), polyacrylamide (PAM), and polyethylene glycol (PEG) [114] have been used to further enhance the performance and applicability of CQDs. These CQDs can be uniformly dispersed in various media, including deionized water and ethanol, facilitating the preparation of diverse anti-counterfeiting materials. Common tools for applying CQDs in anti-counterfeiting include fountain pens, fine brushes, filter paper, and inkjet printers. Techniques used in this field include fluorescent ink, phosphorescent ink, transparent films, and latent fingerprint detection.

In practice, biomass-based CQDs can be applied through various methods, including handwriting, inkjet printing, stamping, spraying, flexographic printing, and screen printing. These techniques ensure that anti-counterfeiting marks remain invisible under daylight but become highly fluorescent under UV light. Thanks to their photostability and biocompatibility, CQD-based anti-counterfeiting materials maintain excellent performance even after long-term storage and multiple uses. Fluorescent anti-counterfeiting technology is widely adopted due to its strong security, fast recognition, and ease of use [146,147]. Traditional fluorescent materials, such as organic fluorescent dyes, suffer from poor stability and resistance

to photobleaching, and some azo-based dyes pose toxicity concerns [148,149]. In contrast, the environmentally friendly nature of biomass-based CQDs minimizes their environmental impact during production and application, making them ideal for large-scale production with strong environmental protection benefits. By leveraging these advantages, the application of biomass-based CQDs in anti-counterfeiting not only enhances the reliability of the technology but also significantly reduces environmental impact, showing great potential for future development. Table 6 summarizes the applications of CQDs in anti-counterfeiting and outlines the characteristics required for effective anti-counterfeiting functionality.

Solvent-based inks release large amounts of environmentally harmful volatile organic compounds (VOCs), making this a major global concern. In contrast, water-based inks do not emit VOCs that contribute to global warming (GW) and are becoming increasingly popular due to their environmentally friendly properties. Previous studies have reported the formulation of water-based flexographic inks using organic molecules as fluorescent pigments [150]. Ullal *et al.* [101] examined the impact of various components (glycerol, surfactants, defoamers, and waxes) in their security inks on the absorbance and emission characteristics of CQDs. The results showed that the addition of wax caused a 17 nm redshift, shifting the emission peak from 473 to 490 nm. The fluorescence intensity of CQDs remained largely unaffected when mixed with glycerol alone, but it decreased steadily when dispersed in surfactants or defoamers, indicating possible interactions with CQD surface groups. Additionally, the dispersion of CQDs in wax significantly reduced fluorescence intensity.

Hong and Yang [102] used ethanol as a solvent, enabling faster drying than water-based inks, with fewer wrinkles and reduced spreading on paper, which is beneficial for anti-counterfeiting applications. No differences in the thickness or surface morphology of the paper were observed, suggesting that the ink penetrated the paper and interacted with its chemical composition, resulting in excellent invisibility of the anti-counterfeiting patterns.

As shown in Figure 6, Shen *et al.* [140] conducted a study to evaluate the potential of CQDs in the field of information encryption, using QR codes (Quick Response codes) as an example. Certain patterns (*e.g.*, ii and iii) were replaced with encryption patterns drawn using CQD-based ink. When the ink was still wet, the encrypted patterns were already difficult to identify (*e.g.*, ii). Once the ink was completely dried, the patterns achieved a fully encrypted effect (*e.g.*, iii). Moreover, under natural light (daylight conditions), the encrypted text within the QR code could not be recognized by smartphone software. However, under 365 nm UV light (*e.g.*, iv), the hidden portions of the QR code became visible and could be decrypted using smartphone software. Furthermore, the study also utilized another type of CQD fluorescent ink (synthesized from oxidized carbon sources) to conduct similar experiments, achieving comparable results (*e.g.*, v to viii). Specifically, only under 365 nm UV light (*e.g.*, viii) could the encrypted patterns and the complete QR code be revealed, successfully enabling the encryption and decryption of information. The experiments demonstrated that both types of CQD-based inks exhibit excellent application potential in fields such as painting, information encryption, and anti-counterfeiting.

Zhang *et al.* [138] synthesized CQDs using spirulina as the carbon source, whose fluorescence color can be dynamically regulated by adjusting the pH of the system. In the experiment, two equal-volume (10 mL) solutions of water, ethanol, and glycerol (mixed in a ratio of 1:3:1) were stirred for 1 h, and their pH values were adjusted to 1.0 and 9.0, respectively. Subsequently, 30 mg of CQDs were dissolved in each solution and stirred for another hour, resulting in red and blue fluorescent inks. These CQD-based nanocomposites were used to fabricate programmable red and blue fluorescent inks capable of complex information encryption and decryption to safeguard critical data. During the encryption-decryption process, triethylamine (TEA) and hydrochloric acid (HCl) were used as encryption and decryption agents, respectively, to achieve pH-induced color switching. For example, Figure 7(a) illustrates the encryption-decryption-re-encryption process of the target protected information “CD” within the word “ENCODE.” Figure 7(b) further shows the conversion of the encoded “CD” information through ASCII binary coding. By switching the CQDs solution color between red and blue under UV light, dynamic data encryption and decryption were successfully achieved. This safe ink demonstrates significant potential in dynamic anti-counterfeiting, multi-level data encryption and decryption, and reversible data encoding under UV light.

Ni *et al.* [114] verified the anti-counterfeiting effect of phosphorescent films using water. When sprayed with water, the blue fluorescence emission remained unchanged, while the green phosphorescence was quenched immediately. The phosphorescence intensity of the CQDs-PVA film decreased significantly under water vapor and recovered once dried. This phenomenon is due to water disrupting the hydrogen bonding between CQDs and PVA, rather than the luminescent centers of the CQDs. The weakened hydrogen bonding reduces system rigidity, enhancing molecular vibrations and rotations. The phosphorescence lifetime of the CQDs-PVA film

Table 6: Anti-counterfeiting applications of biomass-based CQDs

Carbon source	Anti-counterfeiting method/preparation method	Tools/presentation	Characteristics required to realize the anti-counterfeiting function	Ref.
Dwarf banana peel	Fluorescent ink/no additive direct use	Sketch pens, filter paper/handwriting	Excellent dispersibility, high fluorescence performance, photostability, optical transparency, biocompatibility, durability, environmental friendliness, ease of cleaning	[37]
Alkali lignin	Fluorescent ink/no additive direct use	Desktop inkjet printer, non-fluorescent paper/inkjet printing	Chemical stability, High fluorescence performance, green preparation, invisible in daylight	[75]
Phyllanthus acidus (*P. acidus*)	Fluorescent ink/no additive direct use	Pen, filter paper/handwriting	Excellent dispersibility, solubility, high fluorescence performance, optical transparency, durability, environmental friendliness, biocompatibility, ease of cleaning	[87]
Lychee shell	Fluorescent ink/no additive direct use	Pen, filter paper/handwriting	High fluorescence performance, photostability, easy preparation, large-scale production, high cost-efficiency, biocompatibility, low toxicity, chemical stability, hydrophilicity, excellent dispersibility, durability, environmental friendliness, ease of cleaning	[50]
Ganoderma lucidum	Fluorescent ink/homogeneous dispersion of the CD solution	Cotton swabs or fine brushes, filter paper/handwriting	High fluorescence performance, excellent dispersibility, easy preparation	[95]
Tylophora indica plant	Fluorescent ink/addition of styrene with azobisisobutyronitrile	Corrosion-resistant cartridges, non-fluorescent paper/inkjet printing	Thermal stability, humidity stability, photostability, high cost-efficiency, easy preparation	[96]
Pistachio shells	Fluorescent ink/PVA added	Cotton swabs, fine brushes, cellulose paper, ceramics, projection film, plastic, metal, paper/handwriting	Environmental friendliness, photostability, durability, thermal stability	[60]
	Transparent anti-counterfeit (AC) film /PVA added		Flexibility, optical transparency, mechanical stability	
Magnolia flower	Fluorescent ink/filtered through 0.45 and 0.22 μm filters	Non-fluorescent paper/inkjet Printing	High fluorescence performance, stability, excitation dependency	[61]
Parthenium hysterophorus leaf	Fluorescent ink/PVA added	Brushes, glass, leaves, debit cards/handwriting	High fluorescence performance, Stability, excellent dispersibility, environmental friendliness, ease of cleaning, biocompatibility	[62]
	Nanocomposite film/addition of PVA		Optical transparency, flexibility, mechanical stability	
Rhizome of *Acorus calamus*	Fluorescent ink/no additive direct use	Pen, filter paper/handwriting	Chemical stability, high fluorescence performance, high cost-efficiency, environmental friendliness	[63]
Mopan persimmons	Fluorescent inks combined with commercial fluorescent inks (CFI) for double anti-counterfeiting/add sugar	Pens, filter paper, polymethyl methacrylate molds/handwriting	High fluorescence performance, flexibility, easy preparation, environmental friendliness, excitation dependency	[97]
Chinese herbal residues	Fluorescent ink/add ultrapure water	Security paper/cut the paper and put it into fluorescent ink to soak for 2 h and dry, handwriting	High fluorescence performance	[98]
Laurel leaf	Fluorescent ink/add ethanol	Pen, inkjet printer, white paper/handwriting, Printing	High fluorescence performance, chemical stability, photostability, salt tolerance	[64]
	Fluorescent ink/no additive direct use		High fluorescence performance	[99]

(*Continued*)

Table 6: *Continued*

Carbon source	Anti-counterfeiting method/preparation method	Tools/presentation	Characteristics required to realize the anti-counterfeiting function	Ref.
Zanthoxylum bungeanum		The strokes of a Chinese character/ handwriting		
Cordyceps militaris	Waterproof fluorescent ink/add ethanol	Pen, tap water/handwriting	Photostability	[139]
Xanthan gum Oxidized xanthan gum	fluorescent ink/directly encapsulated in two of the most popular neutral pens on the market for drawing and writing.	The strokes of a Chinese character/ handwriting	High fluorescence performance, low toxicity, photostability, biodegradability, environmental friendliness, easy preparation	[140]
Spirulina	PH-responsive bi-illuminated fluorescent inks combined with red commercial inks for multi-layer anti-counterfeiting/add water, ethanol, glycerin	Pen, TEA vapor, HCL vapor, white filter paper/handwriting	High fluorescence performance	[138]
Tapioca starch	Flexographic water-based anti-counterfeiting inks: double emitting inks for document authentication, CD flexographic inks for anti-counterfeiting of flexible electronic products (based on RFID technology)/add deionized water, glycerin, surfactants, defoamers, waxes	UV matting paper/flexographic printing	For document authentication: environmental friendliness, durability, invisible in daylight, photostability For anti-counterfeiting of flexible electronic products: high cost-efficiency, environmental friendliness, easy preparation, large-scale production	[101]
Pine pollen	Fluorescent ink/add glycerin	Non-fluorescent paper, inkjet printer/ inkjet Printing	Easy preparation, high fluorescence performance, Invisible in daylight	[102]
Chitosan	Phosphorescent anti-counterfeit film /PVA, CMC, PAA, PAM, and PEG were added, respectively, named CDs-PVA, CDs-CMC, CDs-PAA, CDs-PAM, and CDs-PEG, respectively. Phosphorescent ink /CDs-PVA as security ink, CDs-PEG as interference ink	CD-based RTP Test Paper (RTP-TP)/ traditional Chinese intaglio stamps, screen printing, inkjet printing	High fluorescence performance, photostability, durability	[114]
Kiwi fruit (*Actinidia deliciosa*) peel	Fluorescent ink/no additive direct use	Fillable sketch pens, filter paper/ handwriting	Excellent dispersibility, high fluorescence performance, photostability, optical transparency, biocompatibility, durability, environmental friendliness, ease of cleaning	[65]
Pigeon manure	Fluorescent ink/add PVA	Filter paper/handwriting	High fluorescence performance, low toxicity, durability, environmental friendliness	[115]
Wasted coffee ground	Fluorescent ink/add PVA	Air compressor, spray gun, Korean paper money/spray	High fluorescence performance, invisible in daylight	[66]
Poplar aspen wood powder	Fluorescent ink/no additive direct use	Commercial pen tubes, non-fluorescent paper, stamps/handwritten, stamped	Stability	[67]
Cherry blossom flowers	Fluorescent ink/no additive direct use	Pen, filter paper/handwriting	Stability, durability, environmental friendliness, ease of cleaning	[68]

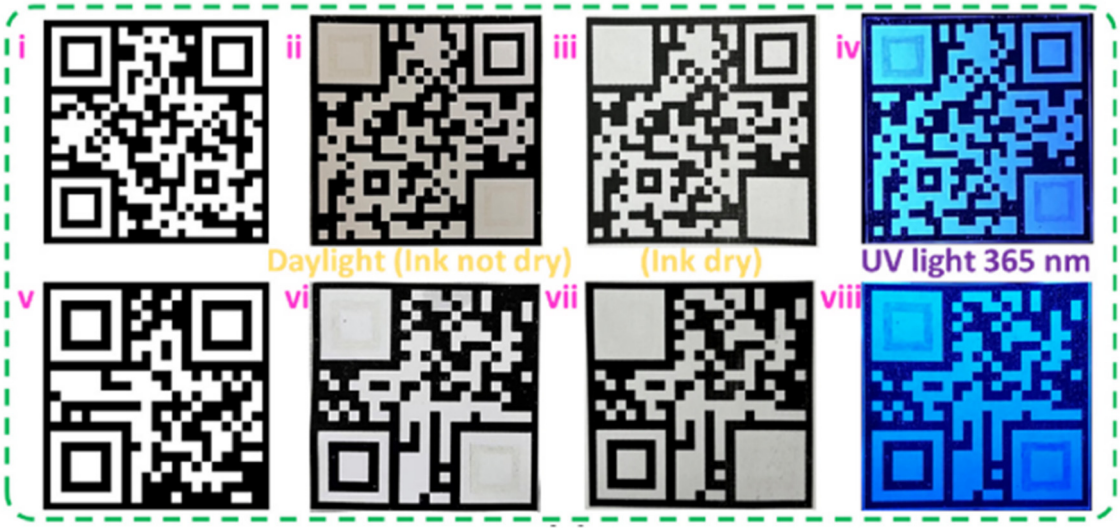

Figure 6: Application of CQD fluorescent ink. - QR Code anti-counterfeiting. Reprinted from Shen *et al.* [140], copyright (2023), with permission from Elsevier.

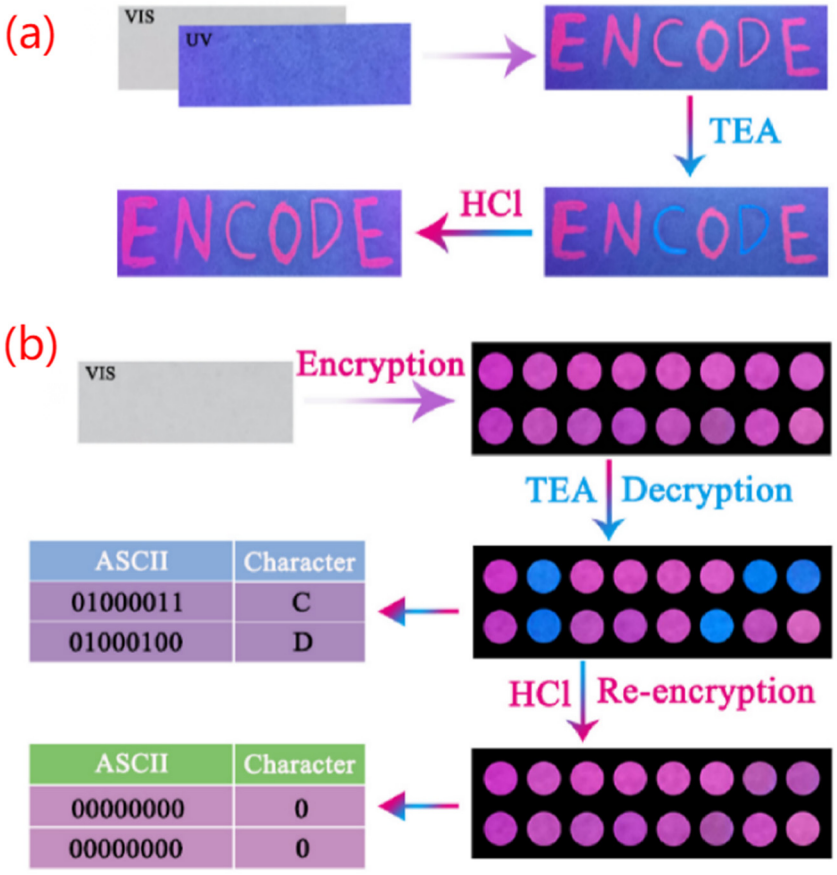

Figure 7: (a) Encryption-decryption-re-encryption process of the protected information “CQDs” within “ENCODE” using pH-responsive CQDs ink. (b) Reversible fluorescence encoding and decoding of “CQDs” based on ASCII binary code. Reprinted from Zhang *et al.* [138], copyright (2023), with permission from Elsevier.

was shortened as water was gradually added to ethanol, destabilizing the excited triplet state and increasing non-radiative transitions.

Ma *et al.* [97] addressed the ACQ process by adding sugar to form CQDs-Sugar complexes. The sugar did not interfere with the excitation-dependent behavior of the CQDs but significantly enhanced emission intensity (by 81% at 0.7 g/mL sugar), increased QY to 13.74%, and extended fluorescence lifetime by 1.73 ns.

Additionally, Krushna *et al.* [62] synthesized CQDs using leaves of Parthenium hysterophorus (silverleaf nightshade) as a carbon source *via* a hydrothermal method. These CQDs were applied in innovative chromogenic fingerprint analysis and anti-counterfeiting applications by integrating latent fingerprint detection, porosity analysis, and the YOLOv8 deep learning algorithm. In this process, computational techniques and deep learning algorithms played a crucial supporting role in CQDs-based experiments. Specifically, deep learning algorithms were employed for the preprocessing of fingerprint images, model training, and predictive analysis (Figure 8a–c), significantly improving the accuracy and efficiency of fingerprint recognition. The experimental results demonstrate that this approach provides robust technical support for the application of CQDs in fingerprint detection, anti-counterfeiting, and related fields.

Sandeep *et al.* [60] synthesized CQDs using pistachio shells as a carbon source through a hydrothermal method and applied them to efficient personal identification by combining latent fingerprint detection techniques and poroscopy. Unlike the approach of Krushna *et al.*, the authors utilized Python programming to enhance fingerprint images, enabling image refinement, feature extraction, and detailed micro-level analysis. This significantly improved detection accuracy and further expanded the application potential of CQDs in the field of anti-counterfeiting. Specifically, Figure 9(a)–(c) presents the fluorescent images of fingerprints collected from various surfaces, including paper, OHP sheets, and steel locks, revealing substantial differences in fingerprint visualization based on surface types. Figure 9(d)–(f) demonstrates the extraction of level-I to -III fingerprint features, including bifurcations, short ridges, cores, and scars, covering a total of 13 micro-level features. The efficient extraction and analysis of these features highlight the effectiveness and precision of combining CQDs with Python-based algorithms for latent

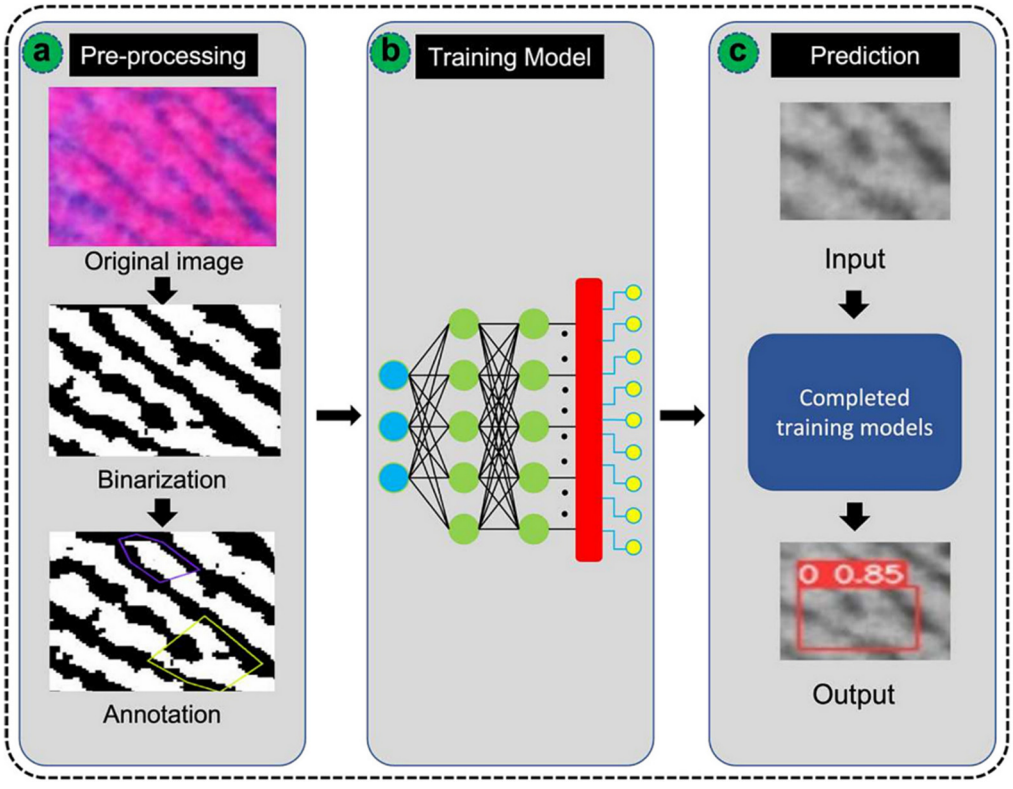

Figure 8: The computational analysis process for fingerprint identification involves three steps: (a) Pre-processing, (b) training model, and (c) prediction process, respectively. Reprinted from Krushna *et al.* [62], copyright (2024), with permission from Elsevier.

fingerprint detection and detailed feature analysis, providing novel insights into the application of CQDs in anti-counterfeiting and personal identification.

3.2 Treatment of dye-contaminated wastewater

In this application, biomass-derived CQDs demonstrate significant advantages in dye wastewater treatment. Biomass CQDs possess excellent environmental properties, with non-toxic basic components and renewable raw material sources, making them a green catalyst. Biomass CQD-based catalysts exhibit high catalytic efficiency and rapid reaction rates, effectively degrading dyes under light irradiation without producing additional harmful by-products. This gives them a clear advantage over traditional methods in wastewater treatment. Furthermore, compared to carbon dots and other nanostructures, biomass CQD composites generally have larger surface areas and porous volumes [151]. This not only enables more dye molecules to be adsorbed onto the catalyst surface, thereby improving catalytic efficiency, but also enhances catalytic performance by extending the electron-hole recombination period. As a result, biomass CQD composites exhibit higher efficiency and stronger performance in photocatalysis, showcasing exceptional catalytic properties and significant potential in dye wastewater degradation.

Smrithi *et al.* [109] synthesized CQDs using zucchini as the carbon source through a hydrothermal method. These CQDs exhibit excellent light absorption properties, low electron-hole recombination rates, and biocompatibility, making them ideal photocatalytic materials. Studies have shown that under visible light irradiation, CQDs can effectively degrade harmful organic dyes in water, such as crystal violet dye. When combined with hydrogen peroxide (H_2O_2), the catalytic degradation efficiency reaches 99.9%. Compared to traditional semiconductor catalysts, CQDs not only demonstrate better dispersion but also offer a simpler synthesis process without the need for additional doping or complex post-treatment steps.

Saafie *et al.* [29] synthesized CQDs from kenaf and demonstrated their excellent photocatalytic degradation performance under optimal synthesis conditions. As shown in Figure 10, although CQDs can remove a portion of methylene

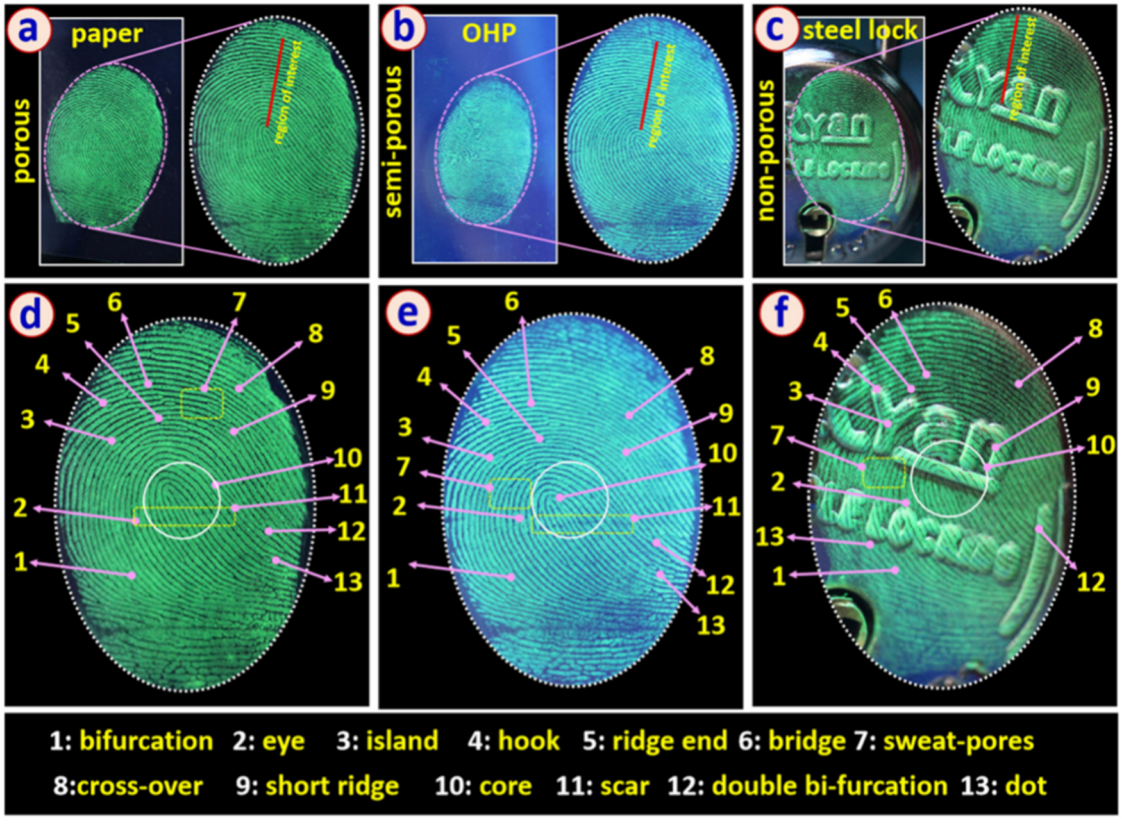

Figure 9: (a–c) Fluorescence images of FPs collected from different surfaces of (paper, OHP sheet, and steel lock). (d–f) Extracted features of levels I–III. Reprinted from Sandeep *et al.* [60], copyright (2024), with permission from Elsevier.

blue (MB) dye through physical adsorption in the absence of light, the removal efficiency is significantly enhanced under light irradiation. Specifically, under 120 min of light exposure, the CQDs can remove up to 90% of MB dye, highlighting their great potential for water pollution treatment. This result indicates that light irradiation significantly enhances the photocatalytic degradation ability of the CQDs, thereby greatly improving the dye removal efficiency. To further investigate the performance of CQDs in the photocatalytic process, the study also conducted a kinetic analysis of the MB degradation reaction. The results showed that the degradation process of the sample followed a pseudo-first-order kinetic model, with a degradation rate constant of 0.023/min, indicating a high decolorization efficiency. The article further proposed a photocatalytic degradation mechanism based on CQDs: when CQDs absorb photons, holes (h^+) are generated in the valence band (VB), and electrons (e^-) are generated in the conduction band. These excited electrons and holes participate in the generation of superoxide radicals (–O_2) and hydroxyl radicals (–OH), which react with water and oxygen, ultimately degrading the MB dye molecules.

Liu *et al.* [152] synthesized CQDs using folic acid as the carbon source. Under different reaction conditions, CQDs exhibited strong degradation ability, achieving nearly 99.69% degradation of nicotine from wastewater within 90 min, indicating their high catalytic performance. Specifically, the reaction temperature significantly affected the catalytic efficiency, with the best catalytic activity observed at 160 and 180°C; the reaction time had less impact on the degradation effect, with a 1 h reaction time being both efficient and energy-saving; increasing nicotine concentration improved the degradation efficiency, and CQDs exhibited excellent catalytic ability in high-concentration nicotine wastewater; the presence of light notably enhanced the degradation efficiency, demonstrating the importance of light in the catalytic reaction; pH value influenced the catalytic effect, with the best degradation performance of CQDs under alkaline and neutral conditions, while acidic conditions led to poorer results; finally, cyclic usage tests showed that CQDs maintained high catalytic activity after six cycles, demonstrating excellent stability and reusability. These results suggest that by optimizing the reaction conditions, CQDs can efficiently and stably treat nicotine wastewater.

Sabet and Mahdavi [153] synthesized CQDs from grass as a carbon source and investigated their application in the treatment of dye-contaminated wastewater. As shown in Figure 11(a)–(f), these CQDs exhibit excellent photocatalytic performance, effectively degrading various dyes such as Acid Blue, Acid Red, Eosin Y, MB, Eriochrome Black T (ECBT), and Methyl Orange under both UV and visible light irradiation. Furthermore, due to their high specific surface area, the CQDs also demonstrate strong adsorption capability for heavy metal ions, with removal efficiencies of 75 and 37% for Cd^{2+} and Pb^{2+}, respectively. Therefore, nitrogen-doped CQDs not only efficiently remove organic dyes but also serve as effective adsorbents for heavy metal ions, offering promising potential for the treatment of dye-contaminated wastewater.

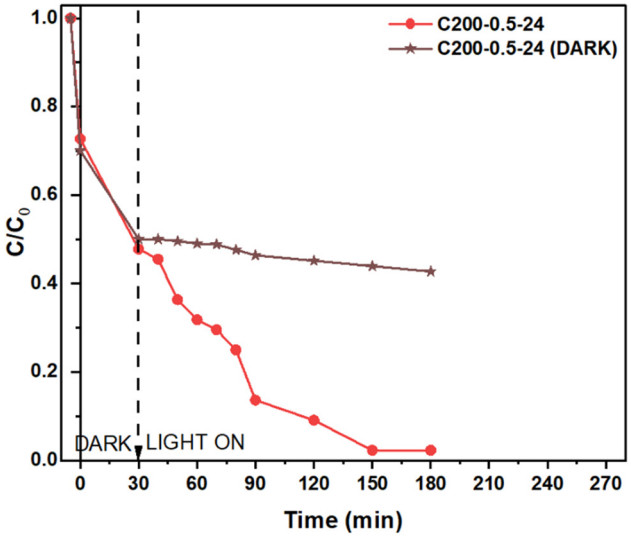

Figure 10: Comparison of the degradation performance of optimized CQDs (C200-0.5-24: 200°C, 0.5 g precursor, 24 h) under visible light irradiation and in total darkness. Reprinted from Saafie *et al.* [29], open access under the Creative Commons license.

3.3 Sensors

Biomass-derived CQDs exhibit significant potential in metal ion sensing due to their excellent fluorescence properties, high stability, high dispersibility, and environmental friendliness. In sensing applications, the fluorescence properties of CQDs can be altered through interactions with metal ions, leading to fluorescence quenching or enhancement. Common mechanisms include static quenching, dynamic quenching, inner filter effect, photo-induced electron transfer, and energy transfer, such as Förster resonance energy transfer, Dexter electron transfer, and surface energy transfer [154]. These mechanisms involve effective electron or energy transfer processes that promote non-radiative electron/hole recombination annihilation, resulting in fluorescence quenching of metal ions. Moreover, the rich surface functionalization of CQDs enables interactions with specific analytes, adjusting their fluorescence properties. Through adsorption or chemical reactions, the surface structure of

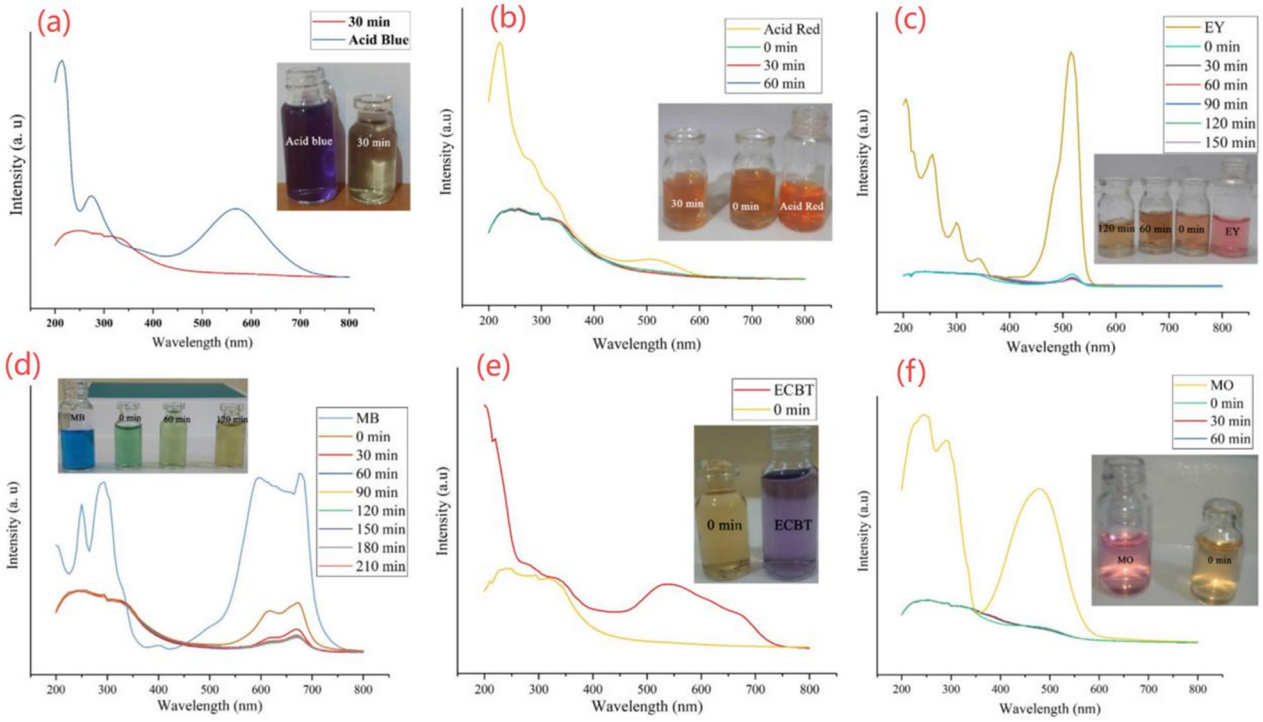

Figure 11: Degradation of different dyes in the presence of CQDs: (a) Degradation of Acid Blue. (b) Degradation of Acid Red. (c) Degradation of Eosin Y. (d) Degradation of MB. (e) Degradation of ECBT. (f) Degradation of Methyl Orange. Reprinted from Sabet and Mahdavi [153], copyright (2019), with permission from Elsevier.

CQDs is altered, allowing for sensitive detection of target analytes. To date, these fluorescence modulation mechanisms (including both quenching and enhancement) have been widely applied in the detection of various molecules and metal ions, further broadening the application prospects of CQDs as sensors in various fields.

CQDs synthesized using rose petals as the carbon source were applied for the detection of the pesticide diazinon [155], demonstrating excellent sensitivity and selectivity. Figure 12(a) illustrates the gradual decrease in the fluorescence intensity of CQDs with increasing diazinon concentrations, indicating that diazinon effectively quenches the fluorescence of CQDs. Figure 12(b) further shows that within the diazinon concentration range of 0.02–10 µM, the change in fluorescence intensity (F_0–F) exhibits a strong linear relationship with diazinon

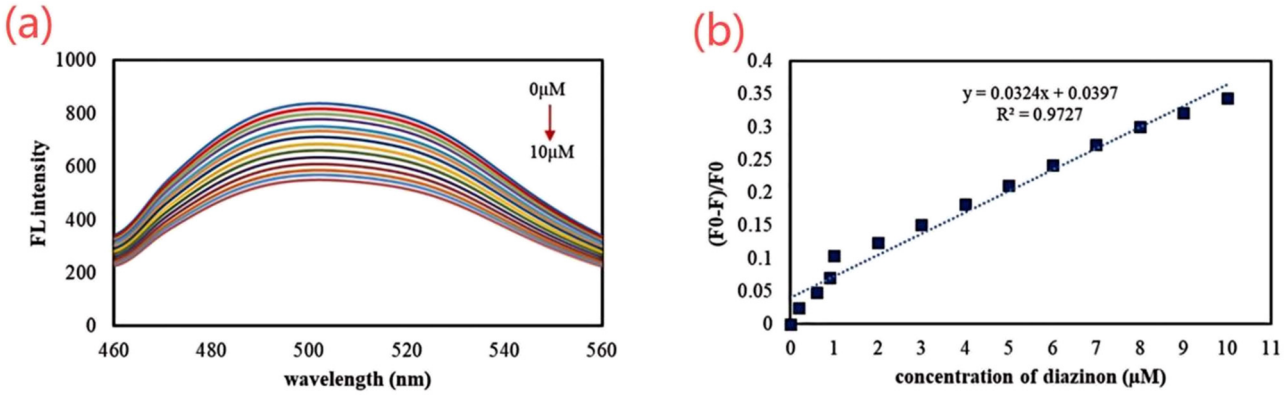

Figure 12: Calibration curve. (a) The change in fluorescence of the CDs with the increase in concentration of Diazinon. (b) A linear correlation of (F_0 – F) values to the concentration of Diazinon in the range from 0.02 to 1 µM. Reprinted from Shekarbeygi *et al.* [155], copyright (2020), with permission from Elsevier.

concentration, with particularly notable linearity in the range of 0.02–1 μM. The study revealed a detection limit of 0.01 μM for this method, with a relative standard deviation (RSD) of 3.5%, indicating high detection sensitivity. Moreover, interference from other pesticides in diazinon detection was minimal, and the recovery rate of diazinon in different water samples ranged from 97.8 to 102.2%, validating the reliability and accuracy of this CQDs-based nanosensor for real sample detection. These results highlight the significant potential of rose-derived CQDs in environmental monitoring, particularly for pesticide residue detection. CQDs synthesized from tobacco as a carbon source were used to differentiate and quantify tetracycline (TC), oxytetracycline (OTC), and chlortetracycline (CTC) [80]. The LODs for TC, OTC, and CTC were 5.18, 6.06, and 14 nM, respectively. Cao [81] synthesized fluorescent Y-CDs through a one-step hydrothermal treatment of yeast powder. These Y-CDs acted as green fluorescent probes for the detection of dopamine (DA), with an LOD of 30 nM and a linear range of 0.05–150 μM. Additionally, the authors synthesized a different type of Y-CDs by adjusting the mass of yeast powder and NaOH concentration. These Y-CDs were used to construct "On-Off-On" sensors for the sensitive and selective detection of Hg^{+} and cysteine, with LODs of 35 and 78.5 nM,

Table 7: Application of CQDs as sensors in metal ion detection

Carbon source	Analyte	Linear range	LOD	Ref.
Rice residue	Fe^{3+}	3.32–32.26 μM	0.7462 μM	[51]
Oxidized cellulose	Fe^{3+}	0–100 μM	1.14 μM	[72]
Corn cob powder	Fe^{3+}	0–120 μM	/	[53]
Cellulose	Fe^{3+}	0.1–6 mM	0.05 mM	[71]
Fish scale of the crucian carp	Fe^{3+}	1–78 μM	0.54 μM	[110]
Phyllanthus acidus (*P. acidus*)	Fe^{3+}	2–25 μM	0.9 μM	[87]
Banana petiole	Fe^{3+}	5–200 nM	0.21 nM	[57]
Cell walls from *Saccharomyces cerevisiae*	Fe^{3+}	0.1–0.5 μM	201 nM	[137]
Northern Shaanxi potatoes	Fe^{3+}	0~500 μM	0.26 μM	[78]
Chionanthus retusus (*C. retusus*) fruit	Fe^{3+}	0–500 μM	70 μM	[93]
Seville orange (*Citrus aurantium*)	Fe^{3+}	33–133 μM	0.53 μM	[94]
Starch fermentation wastewater	Fe^{3+}	0.01–16 μM	3.2 nM	[55]
Phytic acid	Fe^{3+}	10–1,000 μM	0.39 μM	[44]
Lentinus polychrous Lèv	Fe^{3+}	0–2 mM	16 μM	[77]
Apple peel	Fe^{3+}	0.05–300 μM	1.56 μM	[50]
Lychee shell	Fe^{3+}	0–100 μM	/	
Parthenium hysterophorus leaf	Fe^{3+}	0–50 μM	0.14 μM	[62]
Mopan persimmons	Fe^{3+}	0–90 μM	0.324 μM	[97]
Chinese herbal residues	Fe^{3+}	0–80 μM	1.08 μM	[98]
Bombyx mori silk	Fe^{3+}	0.5–4 mM	0.38 mM	[132]
Honeysuckle	Hg^{2+}	0–100 μM	35 nM	[81]
Highland barley	Hg^{2+}	10–160 μM	0.48 μM	[83]
Orange juice	Hg^{2+}	19.94–159.55 μM	0.12 μM	[86]
Pomelo peel	Hg^{2+}	0–40 μM	0.23 nM	[40]
Maojian (a kind of famous green teas)	Hg^{2+}	0.2–60 μM	6 nM	[84]
Spider silk	Hg^{2+}	0–25 μM	5.3 nM	[128]
Citron fruit	Hg^{2+}	0–285 μM	0.15 μM	[103]
Pyrus pyrifolia (pear) fruit	Al^{3+}	0.005–50 μM	2.5 nM	[91]
Quinoa saponin	Co^{2+}	20–150 μM	0.49 μM	[106]
Pigskin	Co^{2+}	0.1–300 μM	68 nM	[134]
Cow milk	Sn^{2+}	0–50 μM	17 μM	[117]
Crab shell	Cd^{2+}	50–250 μM	/	[121]
Wolfberry straw	Cu^{2+}	10–80 nM	2.83 nM	[54]
Butterfly pea (*Cliptoria ternatea*)	Cu^{2+}	1–5 μM	183.33 nM	[157]
Pistachio shells	Cu^{2+}	0–4 μM	0.351 μM	[60]
Fingernail	Cu^{2+}	0–1,000 nM	1 nM	[123]
Xanthan gum	Cr^{6+}	29–357 μM	15.28 μM	[140]
Wool keratin	Cr^{6+}	2.5–50 mM	14.16 nM	[116]
Wool and pig hair	Cr^{6+}	0.05–100 μM	16.8 nM	[133]

respectively. The authors also prepared pH-sensitive fluorescent
H-CDs from honeysuckle as a carbon source. These H-CDs were used to detect the food additive Sunset Yellow (SY), with an LOD of 11 nM and a linear range of 0–40 μM. CQDs synthesized from pre-hydrolyzed lignin served as fluorescent sensors for detecting the illegal food additive Sudan I [73], with an LOD of 0.12 μM. A CQD sensor based on CQDs synthesized from crayfish shells was developed for the detection of 4-nitrophenol [112]. The sensor showed good performance, with recoveries ranging from 95.80 to 103.55% and low RSDs between 0.91 and 4.59%, indicating minimal loss during detection and excellent reproducibility and reliability. A fluorescent sensor for the detection of pyrophosphatase was constructed using CQDs synthesized from willow leaves as the carbon source [46], with recoveries between 98.67 and 102.7%, and RSDs below 5%, demonstrating accurate and reliable results. CQDs synthesized from rambutan seeds were used to selectively and sensitively detect Congo red dye [85] through a fluorescence quenching effect, with a limit of detection (LOD) of 0.035 mM. The sensor was also effective in detecting Congo red in real water samples (tap water and lake water). In addition, John *et al.* synthesized CQDs using rhizomes of *Acorus calamus* [63] as the carbon source for the fluorescence detection of mulberry pigments and the catalytic reduction of rhodamine B and SY. Hu *et al.* synthesized CQDs using *Cordyceps militaris* [139] as the carbon source for the detection of alcohol in alcoholic beverages. Ni *et al.* [114] synthesized CQDs using chitosan as the carbon source and developed a novel room-temperature phosphorescent material, which was used to efficiently, stably, and reliably detect trace amounts of water in various organic solvents. Ye *et al.* [119] synthesized CQDs from chicken bones, using them as fluorescent probes for the detection of laundry detergent. Wu *et al.* [122] synthesized CQDs from chicken cartilage and established an H_2O_2 biosensor, which was applied to glucose detection in human serum.

Moreover, many biomatrix CQDs have been applied as sensors for the detection of metal ions. The fluorescence intensity of CQDs is highly sensitive to metal ions, with most detections based on fluorescence quenching [156]. Table 7 summarizes the applications of CQDs as sensors for metal ion detection, listing their LODs and linear ranges.

3.4 Biomedical research

Biomass-based CQDs have demonstrated significant potential in the field of medical drug delivery due to their exceptional properties. First, CQDs exhibit excellent biocompatibility and high water solubility [158], enabling their rapid dispersion *in vivo* and efficient binding with cells, thereby minimizing toxic side effects. Moreover, their large specific surface area and enhanced cellular uptake capability make them ideal drug carriers [159], allowing for the effective delivery of therapeutic agents to target tissues. The optical properties of CQDs, such as fluorescence and resistance to photobleaching, also enable real-time monitoring during drug delivery, providing valuable insights into drug distribution and therapeutic efficacy. Through targeted delivery, CQDs can reduce side effects on non-target tissues, thereby improving the therapeutic outcomes. Notably, in the treatment of diseases such as cancer, CQDs can function as intelligent drug delivery systems, enhancing treatment efficiency and efficacy.

CQDs synthesized using ginsenoside Rb1 as a carbon source (RBCQDs) have been proposed as a novel nanomedicine with potential applications in the treatment of intracerebral hemorrhage (ICH) [105]. Figure 13 illustrates the synthesis process of RBCQDs and their therapeutic mechanism. High-purity RBCQDs were synthesized *via* a hydrothermal method by mixing ginsenoside Rb1 with ethylenediamine ($C_2H_8N_2$). Compared to traditional iron chelators, RBCQDs exhibit superior antioxidant capacity and iron chelation properties, along with excellent biocompatibility and water solubility. In ICH models, RBCQDs significantly alleviate secondary brain injuries post-ICH by clearing excess iron ions (Fe^{2+} and Fe^{3+}) and reactive oxygen species (ROS) in the meningeal system. Additionally, this nanomedicine reduces oxidative stress and iron-induced cytotoxicity, further promoting the recovery of neurological function. This study provides a new direction for the application of nanomedicine in ICH treatment, while also validating the feasibility of synthesizing CQDs from natural products. It lays a foundation for the development of biomaterials with enhanced therapeutic efficacy and safety for biomedical applications. Curcumin, known for its diverse biological activities, faces limitations in clinical applications due to poor stability, low water solubility, and limited bioavailability. To address these issues, curcumin was loaded onto CQDs synthesized using folic acid as the carbon source, forming a novel nanocomposite [108]. This composite demonstrated significant antibacterial activity against both Gram-negative and Gram-positive bacteria. Moreover, it exhibited pronounced cytotoxicity in cervical cancer cells (HeLa) with high folate receptor expression, while showing no toxic response in hepatocellular carcinoma cells (HepG2) with low folate receptor expression, indicating strong tumor-targeting properties. CQDs synthesized using chlorogenic acid as a carbon source have demonstrated potential as anticancer nanozymes [104]. Figure 14(a) presents

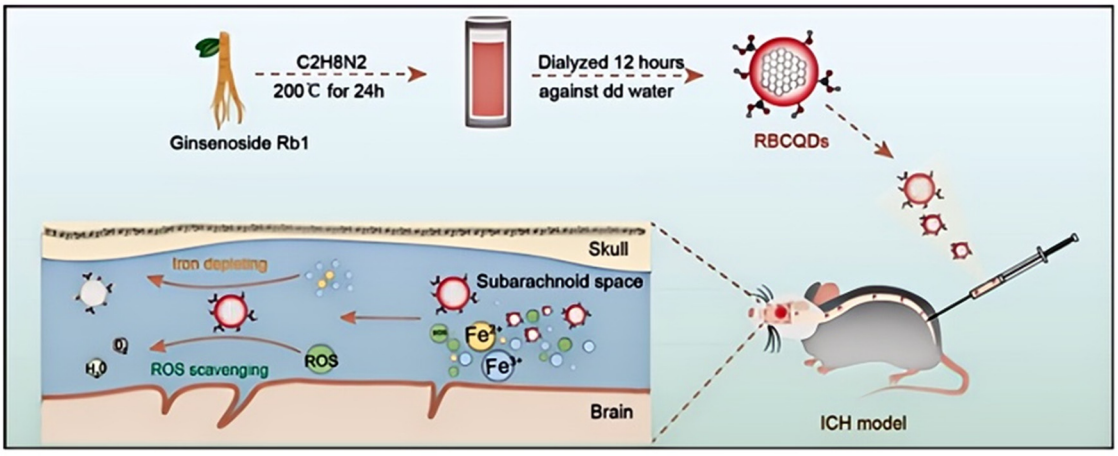

Figure 13: Schematic representation of RBCQDs synthesis and their application in cerebral hemorrhage treatment. Reprinted from Tang *et al.* [105], open access under the Creative Commons license.

tumor images from different experimental groups, where the tumor volume in the CQDs-treated group was significantly smaller than that in the control group and the group treated with the conventional anticancer drug sorafenib. Figure 14(b) compares the tumor weights across different groups on day 12, showing that the tumor weights in the CQDs-treated groups at doses of 5 and 20 mg kg^{-1} were significantly reduced, exhibiting a clear dose-dependent effect. The study revealed that chlorogenic acid-derived CQDs effectively inhibit tumor growth by inducing ferroptosis in tumor cells and activating the tumor immune microenvironment. Additionally, these CQDs exhibited excellent biocompatibility and low toxicity, reducing the side effects commonly associated with conventional anticancer therapies. These findings highlight the promising potential of chlorogenic acid-derived CQDs in tumor immunotherapy and other areas of nanomedicine, providing new insights for the development of more efficient and safer anticancer treatment strategies. CQDs synthesized using cell walls from Saccharomyces cerevisiae as a carbon source exhibited strong antimicrobial activity against both Gram-positive and Gram-negative bacteria [137]. The antibacterial activity is likely attributed to their negative surface charge and ability to generate ROS, which can damage bacterial cell membranes and DNA, leading to bacterial death. Phosphorus doping enhanced ROS generation by introducing additional free electrons, further improving the antibacterial effect. Additionally, these CQDs displayed significant antioxidant activity, highlighting their potential in medical and pharmaceutical applications. CQDs synthesized from *Ganoderma lucidum* [95] as a carbon source generated large amounts of hydroxyl radicals (–OH) through Fenton catalysis, exhibiting super-oxidizing

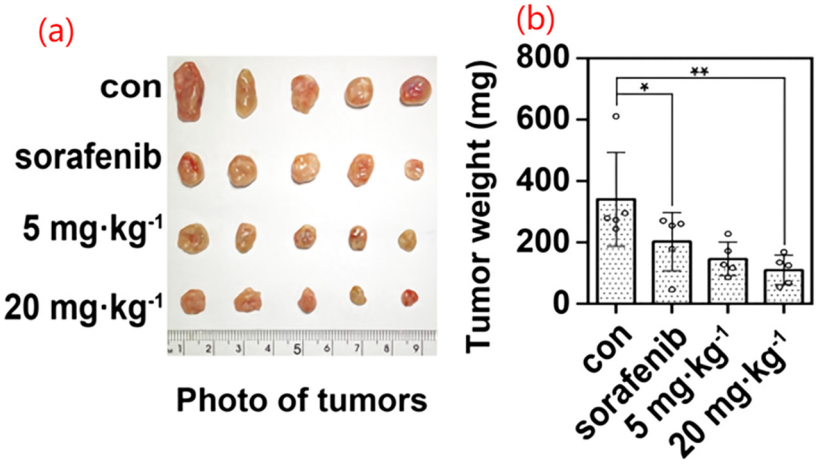

Figure 14: (a) Tumor photos. (b) Tumor weight from different groups at the 12th day after ChA CQDs treatment. Reprinted with permission from Yao *et al.* [104], copyright (2022) American Chemical Society.

capability that induced oxidative stress in tumor cells, ultimately leading to tumor cell apoptosis.

Biomass-based CQDs, with their outstanding properties for medical drug delivery, also exhibit broad application potential in the field of bioimaging. Due to their excellent biocompatibility and high water solubility [160], CQDs can serve as non-toxic imaging probes for cell labeling and disease diagnosis. Their multicolor PL and broad absorption spectrum enable multimodal imaging, providing clear images across various imaging modalities. Moreover, the high photostability and resistance to photobleaching of CQDs allow them to maintain stable brightness during prolonged imaging, further enhancing imaging accuracy and reliability. The low cytotoxicity and biodegradability of CQDs also ensure their safety for long-term applications. Therefore, CQDs not only play a critical role in drug delivery but also serve as ideal probes in bioimaging, offering precise support for disease monitoring and diagnosis. Table 8 summarizes the applications of biomass-based CQDs in bioimaging.

3.5 Environmental sustainability

As biomass-based CQDs, they inherently exhibit low environmental impact and excellent eco-friendly characteristics, making them highly promising for applications in environmental protection and sustainable development. The surface of CQDs is rich in functional groups such as hydroxyl, carboxyl, and amino groups, which facilitate hydrogen transfer pathways, endowing CQDs with remarkable

Table 8: Bioimaging applications of biomass-based CQDs

Carbon source	Mode	Time (h)	Cell/organism	Concentration (mg/mL)	Emission color	Ref.
Banana peel	*In vivo*	24	Nematode worm (*Caenorhabditis elegans*)	0.2	Blue, green, red	[38]
Pakchoi (*Brassica rapa* subsp. *chinensis*)	*In vivo*	6	T24 cell	0.01	Blue, red	[82]
Alkali-soluble Xylan	*In vitro*	6–48	Mouse embryonic stem cell	/	Blue	[69]
Prosopis juliflora leaf	*In vivo*	8	Cryptorchid nematode	1	Green	[49]
Palm kernel shell	*In vitro*	24	HeLa cells, cardiomyocytes, and induced pluripotent stem cells	200	Blue	[43]
Papaya	*In vitro*	3–9	HeLa cells	1	Blue, green	[90]
Oxidized cellulose	*In vivo*	24	Mice	1	Green	[72]
Quinoa saponin	*In vivo*	72	Soybean sprouts	0.8	Blue	[106]
	In vitro	24	HeLa cells	0.15	Blue, green, red	
Lycium ruthenicum	*In vitro*	24	A549 lung cancer cells	1	Blue, green, red	[92]
Pyrus pyrifolia (pear) fruit	*In vitro*	6	*Bacillus subtilis*	0.01	Blue, green	[91]
Chionanthus retusus (*C. retusus*) fruit	*In vitro*	2, 6	Yeast strains (*Candida albicans* 6 h and *Cryptococcus neoformans* 2 h)	0.01	Blue	[93]
Orange juice	*In vitro*	24	Human THP-1 macrophages	0.2–25	Blue	[86]
Phytic acid	*In vitro*	28	HeLa cells	0.2	Blue	[44]
The unripe fruit of *Prunus persica* (peach)	*In vitro*	24	MDA-MB-231 cells	0.01	Blue	[89]
Honeysuckle	*In vitro*	24	HeLa cells	0.1	Blue	[81]
Wheat straw	*In vitro*	12	*Escherichia coli*	0.2	Blue, green	[52]
	In vivo		Cryptorchid nematode			
Phyllanthus acidus (*P. acidus*)	*In vitro*	2	Pseudohyphae	0.01	Blue	[87]
		24	Clone 9 rat hepatocytes	0–0.1	Blue, green, red	
Chlorogenic acid	*In vitro*	0.5	HepG2 cells	0.1	Blue	[104]
Banana petiole	*In vitro*	2, 6, 24	Banana leaf cell	0.5	Blue	[57]
Mussel	*In vitro*	24	HepG2 cells	6	Blue	[120]
	In vivo	48	Zebrafish larva	/		
Pork skin collagen	*In vitro*	24	Human fetal ventricular cardiomyocytes	0.5	Blue	[129]

antioxidant properties that mitigate the negative effects of environmental stress on plants [107]. Moreover, the unique optical properties of CQDs, particularly their UV fluorescence, enable them to regulate light capture and energy conversion in plant photosynthesis, thereby improving plants' efficiency in utilizing light energy. The potential of CQDs in environmental sustainability has been extensively explored, especially in the context of green energy conversion, where they demonstrate exceptional catalytic performance and minimal environmental impact. Therefore, biomass-based CQDs not only promote plant growth and enhance stress resistance but also offer innovative solutions for environmental protection and sustainable energy production.

As shown in Figure 15, Johny *et al.* [45] conducted an environmental impact analysis of the CQDs synthesis process using the life cycle assessment approach, specifically employing the ReCiPe2016 midpoint (H) method. The results revealed that citric acid, commonly used in traditional CQDs synthesis, is the primary contributor to many environmental impact categories. However, by utilizing biomass sources, such as eucalyptus leaves, as the carbon precursor, the reliance on citric acid can be significantly reduced, thereby mitigating the environmental impacts of the synthesis process. The figure illustrates that compared to CQDs synthesized without biomass, the use of eucalyptus leaves as the carbon source leads to substantial improvements across multiple environmental impact categories, such as GW stratospheric ozone depletion (SOD), and LU. Notably, the impacts on LU and ozone layer depletion are reduced by nearly half, highlighting the significant sustainability advantages of biomass-based CQDs synthesis strategies. Furthermore, the study indicated that using biomass not only decreases the overall environmental impact but also enhances resource efficiency in terms of WC and mineral resource scarcity. These findings suggest that integrating biomass as a raw material and optimizing CQDs synthesis processes can simultaneously achieve high-performance material production and significant reductions in environmental impact. This provides valuable guidance for advancing green chemistry synthesis technologies and promoting sustainable development.

CQDs synthesized from willow wood powder as a carbon source have demonstrated significant potential in enhancing photosynthesis [59]. CQDs effectively capture UV light and convert it into blue light, thereby improving the efficiency of chloroplasts in utilizing light energy. Figure 16 illustrates the mechanism by which CQDs facilitate light energy capture and enhance chloroplast photosynthesis. By interacting with Photosystem II, CQDs convert light energy into chemical energy, driving the generation of NADPH and the synthesis of ATP, thus enhancing the overall efficiency of photosynthesis. Experimental results showed that chlorophyll content in legume leaves treated with CQDs significantly increased, particularly at low concentrations, where nitrogen-doped CQDs exhibited superior enhancement effects. This effect is attributed to the critical role of nitrogen-doped CQDs in light harvesting and energy conversion. This study provides a theoretical foundation for the development of CQD-based agricultural yield enhancement technologies while highlighting the

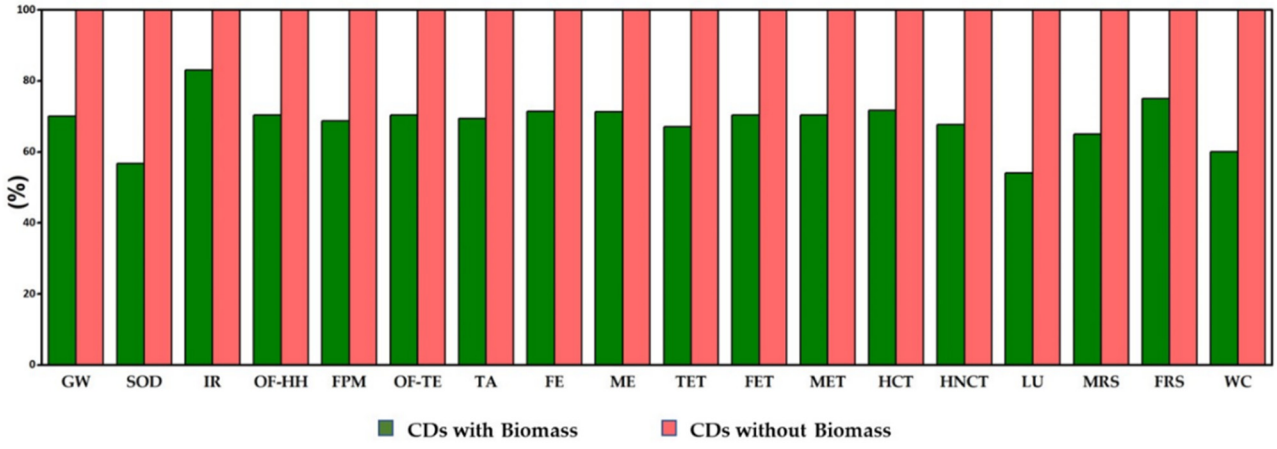

Figure 15: Comparison of environmental impact analysis of hydrothermally synthesized CQDs with and without biomass using the ReCiPe2016 midpoint (H) method. Impact categories include GW, SOD, ionizing radiation, ozone formation-human health (OF-HH), fine particulate matter formation (FPM), ozone formation-terrestrial ecosystem (OF-TE), terrestrial acidification, freshwater eutrophication, marine eutrophication, terrestrial ecotoxicity, freshwater ecotoxicity, marine ecotoxicity, human carcinogenic toxicity, human non-carcinogenic toxicity, LU, mineral resource scarcity, fossil resource scarcity, and water consumption (WC). Reprinted from Johny *et al.* [45], open access under the Creative Commons license.

potential application of biomass-derived functional CQDs in promoting photosynthesis. CQDs synthesized from proanthocyanidins as a carbon source demonstrated significant efficacy in alleviating salt stress in rice plants [107]. Studies revealed that rice seedlings treated with these CQDs exhibited a substantial increase in fresh weight and chlorophyll content under salt stress conditions, indicating their ability to mitigate the adverse effects of salt stress. Moreover, these CQDs enhanced the antioxidant capacity of the plants by increasing antioxidant enzyme activity in the rice seedlings, reducing oxidative damage. Waste Cooking Oil (WCO) refers to the oil discarded during cooking processes, and once released into water bodies, it can cause significant environmental pollution. For instance, just 1 L of WCO can contaminate up to 500,000 L of natural water. Therefore, the recycling and treatment of WCO are of utmost importance. Kalpana *et al.* [141] utilized exopolysaccharides as a carbon source to synthesize CQDs and applied them in biodiesel production. Experimental results demonstrated that CQDs derived from exopolysaccharides exhibit excellent catalytic performance, effectively enhancing the conversion efficiency of WCO into biodiesel. Compared to traditional catalysts, CQD catalysts show superior stability and lower environmental impact. Moreover, when combined with sodium hydroxide and other base catalysts, the biodiesel yield can reach 96.97%. Thus, the application of CQDs derived from exopolysaccharides in biodiesel production not only improves conversion efficiency but also provides a more environmentally friendly alternative.

4 Summary and future prospects

This review systematically summarizes the current progress and application prospects of biomass-based CQDs synthesized *via* hydrothermal methods. Due to their low cost, environmental friendliness, and excellent biocompatibility, biomass-based CQDs have shown great potential in various fields such as anti-counterfeiting, wastewater treatment, and biomedicine. Different types of biomass (plant, animal, and microbial sources) serve as carbon precursors for the hydrothermal synthesis of CQDs, each with distinct characteristics and advantages.

Plant-based carbon sources, such as plant waste (*e.g.*, lignin and cellulose), are ideal for CQDs synthesis due to their wide availability, low cost, and environmental benefits. These plant-based precursors provide an abundant carbon source and unique electronic properties, enhancing the photostability and fluorescence performance of CQDs, which are widely utilized in anti-counterfeiting and environmental remediation. Animal-based carbon sources, such as crayfish shells and chicken feathers, are rich in nitrogen, which facilitates nitrogen doping in CQDs, thereby improving their photostability and optical properties. These features

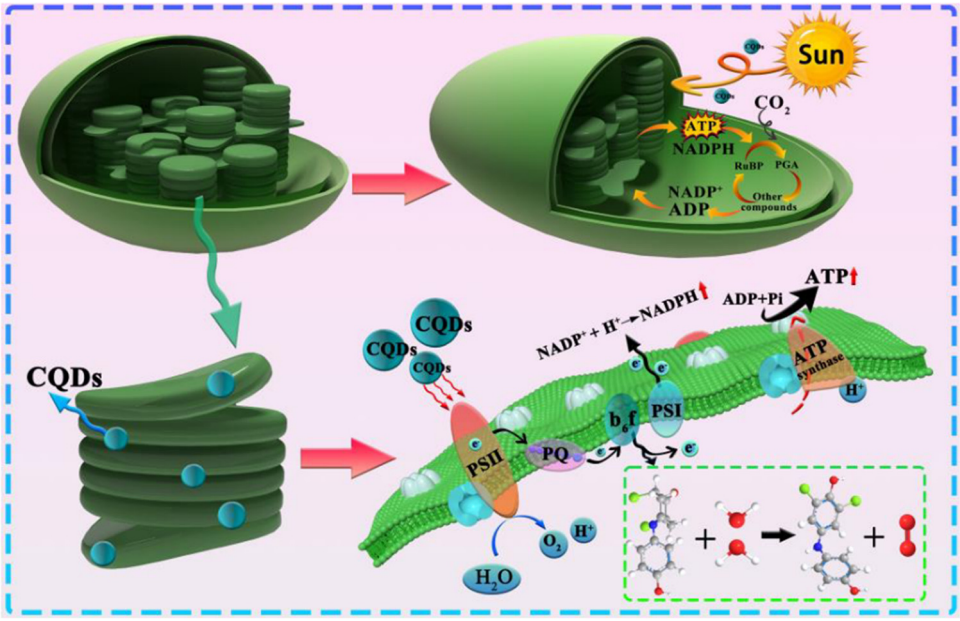

Figure 16: Schematic diagram of CQDs promoting light energy capture by chloroplasts to enhance photosynthesis. Reprinted from Fu *et al.* [59], open access under the Creative Commons license.

make CQDs synthesized from animal sources highly promising for applications in sensors, catalysts, and drug delivery systems. Microbial-based carbon sources, particularly yeast cell walls and yeast powder, contribute polysaccharides, proteins, and lipids during the hydrothermal synthesis process, endowing CQDs with superior biocompatibility and surface functionalization capabilities. This significantly enhances their application potential in bioimaging, sensing, and drug delivery.

This review also highlights examples of biomass-based CQD applications in anti-counterfeiting, wastewater treatment, sensors, biomedicine, and environmental sustainability. In the anti-counterfeiting field, biomass-based CQDs have become a vital component of anti-counterfeiting materials due to their excellent fluorescence properties, photostability, and biocompatibility. CQDs are used in various anti-counterfeiting technologies such as fluorescent inks, transparent films, and fingerprint detection, offering high concealment, photostability, and resistance to bleaching, making them suitable for large-scale production. In wastewater treatment, biomass-based CQDs demonstrate high photocatalytic activity, effectively degrading harmful organic dyes in water, with significantly enhanced catalytic efficiency under light exposure. This showcases their sustainability and low environmental impact. In sensor applications, the fluorescence properties of biomass-based CQDs enable sensitive detection of metal ions and pesticides, highlighting their potential for environmental monitoring and food safety applications. In the biomedical field, biomass-based CQDs, with their excellent biocompatibility and optical properties, have been employed in drug delivery and bioimaging, showing potential as critical materials in nanotheranostics. Moreover, biomass-based CQDs have demonstrated potential in environmental sustainability, including promoting plant growth, enhancing stress resistance, and improving photosynthetic efficiency. With the continuous optimization of synthesis techniques and advancements in application research, biomass-based CQDs are poised to provide green and sustainable solutions across multiple fields, paving the way for broader industrial and scientific applications.

Although biomass-based CQDs exhibit promising potential across various applications, several challenges remain to be addressed. To begin with, while the hydrothermal method is commonly used for CQDs synthesis, it still faces issues such as harsh temperature and pressure conditions, low yield, and inconsistent quality. To enhance synthesis efficiency and yield, researchers could explore optimized reaction conditions, introduce novel catalysts, or adopt milder reaction parameters. Additionally, the issue of batch-to-batch variability needs to be resolved. Future research should focus on developing controllable and highly reproducible production processes and establishing standardized quality criteria to ensure product consistency during large-scale production. Furthermore, although biomass-based CQDs exhibit excellent biocompatibility in biomedical applications, their long-term *in vivo* metabolism and biodegradability remain insufficiently evaluated. As their use in drug delivery and cell labeling increases, further investigations are necessary to assess their toxicity, immune response, and long-term exposure safety to ensure their effectiveness and safety in medical applications.

In wastewater treatment, biomass-based CQDs possess significant photocatalytic performance; however, their catalytic efficiency is limited by surface defects, particle size heterogeneity, and electron-hole recombination. To improve photocatalytic efficiency, strategies such as doping, surface modification, or incorporating composite materials could be employed to enhance electron transfer capabilities and improve catalytic stability and efficiency in practical applications. Moreover, the development of novel photocatalytic systems could further enhance the application of CQDs in wastewater treatment.

In the biomedical field, despite the promising performance of CQDs in drug delivery and bioimaging, deep-tissue imaging remains limited due to tissue absorption and scattering. To overcome this limitation, optimizing the size, optical properties, and surface functionalization of CQDs could improve their imaging capabilities in deep tissues. Additionally, integrating advanced imaging technologies, such as near-infrared imaging, could further enhance imaging precision, advancing the application of CQDs in medical diagnostics.

In environmental sustainability, biomass-based CQDs have demonstrated potential due to their eco-friendly characteristics. However, their relatively weak antioxidant performance and hydrogen donation capacity may limit broader applications. Enhancing these properties through surface modification, such as introducing more functional groups (*e.g.*, amino, carboxyl), could improve their antioxidant capacity and hydrogen donation ability. Furthermore, as biomass-based CQDs see broader use, their long-term environmental impacts and biodegradability require further evaluation to ensure their sustainability and ecological safety in extended applications.

In the field of anti-counterfeiting applications, biomass-based CQDs have emerged as highly promising materials due to their unique fluorescent properties and excellent biocompatibility. These CQDs provide multicolor fluorescence output and exhibit superior characteristics in terms of water solubility, eco-friendliness, and low toxicity compared to traditional organic fluorescent dyes.

Consequently, biomass-based CQDs offer significant advantages for use in anti-counterfeiting markers. However, despite their potential, maintaining long-term stability under real-world conditions remains a major challenge. In practical applications, CQDs are exposed to factors such as UV light, temperature, humidity, and bleaching agents, which can lead to the degradation of their fluorescent properties. This is particularly critical for anti-counterfeiting materials used in documents and passports, which are often subjected to harsh environmental conditions (*e.g.*, intense UV radiation, high temperatures, and humidity). Prolonged exposure to such conditions may result in fluorescence quenching or fading, thereby compromising their anti-counterfeiting effectiveness. Future research should therefore prioritize addressing the issue of long-term stability, particularly under varying climatic conditions, such as temperature, humidity, light exposure, and resistance to bleaching agents. An effective strategy to enhance CQD stability involves surface modification or the incorporation of composite materials to improve resistance to photobleaching, chemical stability, and UV-aging. For instance, doping CQDs with other elements or employing polymer encapsulation techniques could enhance their durability in extreme environments. Beyond material durability, anti-counterfeiting technologies also require materials with multiple security features. In the case of documents and passports, for example, anti-counterfeiting materials must not only exhibit fluorescent properties but also provide color diversity and unique characteristics under different excitation wavelengths to effectively prevent replication by counterfeiters. Additionally, properties such as adhesion, durability, and magnetism must undergo rigorous testing. These properties should be verified through various evaluation methods, such as adhesion tests, durability tests, optical property assessments, and magnetic property evaluations, to ensure the long-term effectiveness of anti-counterfeiting performance. Another critical consideration in practical applications is the printability of anti-counterfeiting materials. Ensuring high-resolution and clear printing during production is essential to prevent anti-counterfeiting markers from being easily replicated or tampered with. Achieving this requires the use of high-quality printing technologies to maintain the clarity and precision of patterns and markers. Furthermore, field tests and third-party certifications play a crucial role in ensuring that the selected materials perform effectively under real-world conditions, thereby reducing the occurrence of counterfeit products. From an economic perspective, biomass-based CQDs, as eco-friendly materials, also offer cost advantages compared to traditionally synthesized CQDs. Biomass resources are abundant, renewable, and have low raw material costs. During the synthesis of biomass-based CQDs, agricultural waste, plant residues, and other low-cost materials can be utilized, reducing production costs while contributing to sustainable development. This makes biomass-based CQDs an ideal choice for anti-counterfeiting applications, as they not only provide excellent anti-counterfeiting performance but also reduce production costs.

In conclusion, while biomass-based CQDs exhibit immense potential across various application fields, further research is needed to address challenges in production processes, performance enhancement, and safety. By optimizing synthesis methods, improving yield and quality, and tackling specific application-related issues, biomass-based CQDs are poised to achieve broader applications and drive their commercialization across diverse industries.

Acknowledgments: The authors would like to thank Professors Zhang Yan and Zhang Mei from China People's Police University for their valuable support and insightful discussions that contributed to the development of this manuscript.

Funding information: The authors gratefully acknowledge the financial support from the National Natural Science Foundation of China (NSFC) (52071003), High-Level Talent University-Level Special Research Program of the China People's Police University (BSKYZX202401), and Graduate Science and Technology Innovation Program of the China People's Police University (YJSKC2503).

Author contributions: Project proposal: Xiaodong Wang and Sudan Liu. Research design and guidance: Xiaodong Wang and Sudan Liu. Investigation: Xiangping Xu, Wang Du, Zhongxiang Qiao, and Yabin Zhou. Writing – original draft preparation: Xiangping Xu and Xiaodong Wang. Writing – review and editing: Xiangping Xu, Xiaodong Wang, and Wang Du. All authors have accepted responsibility for the entire content of this manuscript and approved its submission.

Conflict of interest: The authors state no conflict of interest.

Data availability statement: Data sharing is not applicable to this article as no datasets were generated or analysed during the current study.

References

[1] Bourlinos AB, Stassinopoulos A, Anglos D, Zboril R, Georgakilas V, Giannelis EP. Photoluminescent carbogenic dots. Chem Mater. 2008;20(14):4539–41.

[2] Xu X, Ray R, Gu Y, Ploehn HJ, Gearheart L, Raker K, et al. Electrophoretic analysis and purification of fluorescent single-walled carbon nanotube fragments. J Am Chem Soc. 2004;126(40):12736–7.
[3] Doñate-Buendia C, Torres-Mendieta R, Pyatenko A, Falomir E, Fernández-Alonso M, Mínguez-Vega G. Fabrication by laser irradiation in a continuous flow jet of carbon quantum dots for fluorescence imaging. ACS Omega. 2018;3(3):2735–42.
[4] Hou Y, Lu Q, Deng J, Li H, Zhang Y. One-pot electrochemical synthesis of functionalized fluorescent carbon dots and their selective sensing for mercury ion. Anal Chim Acta. 2015;866:69–74.
[5] Wang X, Feng Y, Dong P, Huang J. A mini review on carbon quantum dots: preparation, properties, and electrocatalytic application. Front Chem. 2019;7:671.
[6] Wu Y, Liu Y, Yin J, Li H, Huang J. Facile ultrasonic synthesized NH2-carbon quantum dots for ultrasensitive Co2+ ion detection and cell imaging. Talanta. 2019;205:120121.
[7] Su JX. Preparation of nanomaterials with different dimensions and their application in detection and electrocatalytic nitrate reduction [dissertation]. Gansu, China: Lanzhou University; 2021. Chinese.
[8] Singh P, Kumar S, Kumar K. Biogenic synthesis of Allium cepa derived magnetic carbon dots for enhanced photocatalytic degradation of methylene blue and rhodamine B dyes. Biomass Convers Biorefin. 2025;15(1):869–87.
[9] Xie Y, Kocaefe D, Chen C, Kocaefe Y. Review of research on template methods in preparation of nanomaterials. J Nanomater. 2016;2016(1):2302595.
[10] Anwar S, Ding H, Xu M, Hu X, Li Z, Wang J, et al. Recent advances in synthesis, optical properties, and biomedical applications of carbon dots. ACS Appl Bio Mater. 2019;2(6):2317–38.
[11] Zuo P, Lu X, Sun Z, Guo Y, He H. A review on syntheses, properties, characterization and bioanalytical applications of fluorescent carbon dots. Mikrochim Acta. 2016;183:519–42.
[12] Javed M, Saqib AN, Ali B, Faizan M, Anang DA, Iqbal Z, et al. Carbon quantum dots from glucose oxidation as a highly competent anode material for lithium and sodium-ion batteries. Electrochim Acta. 2019;297:250–7.
[13] Zheng XT, Ananthanarayanan A, Luo KQ, Chen P. Glowing graphene quantum dots and carbon dots: properties, syntheses, and biological applications. Small. 2015;11(14):1620–36.
[14] Ling L, Zhu Z, Shen H, Cheng R, Ye HG, Li Q, et al. One-step facile synthesis of fluorescent carbon dots via magnetic hyperthermia method. Ind Eng Chem Res. 2020;59(11):4968–76.
[15] Li CX, Yu C, Wang CF, Chen S. Facile plasma-induced fabrication of fluorescent carbon dots toward high-performance white LEDs. J Mater Sci. 2013;48:6307–11.
[16] Liu WJ, Tian K, He YR, Jiang H, Yu HQ. High-yield harvest of nanofibers/mesoporous carbon composite by pyrolysis of waste biomass and its application for high durability electrochemical energy storage. Environ Sci Technol. 2014;48(23):13951–9.
[17] Sun W, Sun Y, Hong X, Zhang Y, Liu C. Research on biomass waste utilization based on pollution reduction and carbon sequestration. Sustainability. 2023;15(5):4535.
[18] Sharma HB, Sarmah AK, Dubey B. Hydrothermal carbonization of renewable waste biomass for solid biofuel production: A discussion on process mechanism, the influence of process parameters, environmental performance and fuel properties of hydrochar. Renew Sust Energy Rev. 2020;123:109761.
[19] McIlveen-Wright DR, Huang Y, Rezvani S, Mondol JD, Redpath D, Anderson M, et al. A techno-economic assessment of the reduction of carbon dioxide emissions through the use of biomass co-combustion. Fuel. 2011;90(1):11–8.
[20] Williams JM, Bourtsalas AC. Assessment of co-gasification methods for hydrogen production from biomass and plastic wastes. Energies. 2023;16(22):7548.
[21] Sri Shalini S, Palanivelu K, Ramachandran A, Raghavan V. Biochar from biomass waste as a renewable carbon material for climate change mitigation in reducing greenhouse gas emissions—a review. Biomass Convers Biorefin. 2021;11(5):2247–67.
[22] Shi J, Zhang R, Liu X, Zhang Y, Du Y, Dong H, et al. Advances in multifunctional biomass-derived nanocomposite films for active and sustainable food packaging. Carbohydr Polym. 2023;301:120323.
[23] Xu Y, Wang B, Zhang M, Zhang J, Li Y, Jia P, et al. Carbon dots as a potential therapeutic agent for the treatment of cancer-related anemia. Adv Mater. 2022;34(19):2200905.
[24] Moradi M, Molaei R, Kousheh SA, Guimarães JT, McClements DJ. Carbon dots synthesized from microorganisms and food by-products: active and smart food packaging applications. Crit Rev Food Sci Nutr. 2023;63(14):1943–59.
[25] Wang B, Tang W, Lu H, Huang Z. Hydrothermal synthesis of ionic liquid-capped carbon quantum dots with high thermal stability and anion responsiveness. J Mater Sci. 2015;50:5411–8.
[26] Zhao C, Jiao Y, Hua J, Yang J, Yang Y. Hydrothermal synthesis of nitrogen-doped carbon quantum dots as fluorescent probes for the detection of dopamine. J Fluoresc. 2018;28:269–76.
[27] Rani N, Singh P, Kumar S, Bhankar V, Kumar D, Kumar K. An introduction to carbon quantum dots. In: Kumar V, Singh P, Singh DK, editors. Green carbon quantum dots. Singapore: Springer; 2024. p. 1–24.
[28] Wongso V, Sambudi NS, Sufian S, Isnaeni. The effect of hydrothermal conditions on photoluminescence properties of rice husk-derived silica-carbon quantum dots for methylene blue degradation. Biomass Convers Biorefin. 2021;11:2641–54.
[29] Saafie N, Sambudi NS, Wirzal MDH, Sufian S. Effect of hydrothermal conditions on kenaf-based carbon quantum dots properties and photocatalytic degradation. Separations. 2023;10(2):137.
[30] Wang L, Weng S, Su S, Wang W. Progress on the luminescence mechanism and application of carbon quantum dots based on biomass synthesis. RSC Adv. 2023;13(28):19173–94.
[31] Wareing TC, Gentile P, Phan AN. Biomass-based carbon dots: current development and future perspectives. ACS Nano. 2021;15(10):15471–501.
[32] Gan J, Chen L, Chen Z, Zhang J, Yu W, Huang C, et al. Lignocellulosic biomass-based carbon dots: synthesis processes, properties, and applications. Small. 2023;19(48):2304066.
[33] Oladzadabbasabadi N, Dheyab MA, Nafchi AM, Ghasemlou M, Ivanova EP, Adhikari B. Turning food waste into value-added carbon dots for sustainable food packaging application: a review. Adv Colloid Interface Sci. 2023;321:103020.
[34] Fang M, Wang B, Qu X, Li S, Huang J, Li J, et al. State-of-the-art of biomass-derived carbon dots: Preparation, properties, and applications. Chin Chem Lett. 2024;35(1):108423.
[35] Singh P, Rani N, Kumar S, Kumar P, Mohan B, Bhankar V, et al. Assessing the biomass-based carbon dots and their composites for photocatalytic treatment of wastewater. J Clean Prod. 2023;413:137474.

[36] Singh P, Rani N, Kumar K, Kumar S, Kumar P, Bhankar V. Degradation of organic pollutants present in water using green synthesized carbon quantum dots. In: Kumar V, Singh P, Singh DK, editors. Green carbon quantum dots. Singapore: Springer; 2024. p. 209–35.
[37] Atchudan R, Edison TN, Perumal S, Muthuchamy N, Lee YR. Hydrophilic nitrogen-doped carbon dots from biowaste using dwarf banana peel for environmental and biological applications. Fuel. 2020;275:117821.
[38] Atchudan R, Edison TN, Shanmugam M, Perumal S, Somanathan T, Lee YR. Sustainable synthesis of carbon quantum dots from banana peel waste using hydrothermal process for in vivo bioimaging. Phys E Low Dimens Syst Nanostruct. 2021;126:114417.
[39] González-Martínez GA, García LG, Frutis-Murillo M, Martínez-Torres P, López-Meza JE, Rosas G. Hydrothermal synthesis of carbon quantum dots from Citrus limetta peels: Exploration of pH sensing, non-hemolytic activity and thermoluminescent properties. Mater Lett. 2024;373:137119.
[40] Lu W, Qin X, Liu S, Chang G, Zhang Y, Luo Y, et al. Economical, green synthesis of fluorescent carbon nanoparticles and their use as probes for sensitive and selective detection of mercury (II) ions. Anal Chem. 2012;84(12):5351–7.
[41] Han L, Guo Y, Zhang H, Wang Z, Zhang F, Wang Y, et al. Preparation of carbon quantum dot fluorescent probe from waste fruit peel and its use for the detection of dopamine. RSC Adv. 2024;14(3):1813–21.
[42] Ferjani H, Abdalla S, Oyewo OA, Onwudiwe DC. Facile synthesis of carbon dots by the hydrothermal carbonization of avocado peels and evaluation of the photocatalytic property. Inorg Chem Commun. 2024;160:111866.
[43] Abu N, Chinnathambi S, Kumar M, Etezadi F, Bakhori NM, Zubir ZA, et al. Development of biomass waste-based carbon quantum dots and their potential application as non-toxic bioimaging agents. RSC Adv. 2023;13(40):28230–49.
[44] Xing Y, Yang M, Chen X. Fabrication of P and N Co-doped carbon dots for Fe3 + detection in serum and lysosomal tracking in living cells. Biosensors. 2023;13(2):230.
[45] Johny A, Pinto da Silva L, Pereira CM, Esteves da Silva JC. Sustainability assessment of highly fluorescent carbon dots derived from eucalyptus leaves. Environments. 2024;11(1):6.
[46] He W, Wu S, Cui R, Zhang J, Lim SF. Preparation of carbon quantum dots based on willow leaves as raw materials and their use as fluorescent probes for high-sensitivity detection of pyrophosphatase. J Phys Conf Ser. 2024;2679(1):012009.
[47] Tariq M, Shivalkar S, Hasan H, Sahoo AK, Sk MP. Manganese doping in biomass derived carbon dots amplifies white light-induced antibacterial activity. ACS Omega. 2023;8(51):49460–6.
[48] Shi H, Li C, Ke X, Cai Y, Qian S, Wu L, et al. Color integration in biomass-derived carbon dots to realize one-step white light. Green Chem Lett Rev. 2023;16(1):2214178.
[49] Prathap N, Balla P, Shivakumar MS, Periyasami G, Karuppiah P, Ramasamy K, et al. Prosopis juliflora hydrothermal synthesis of high fluorescent carbon dots and its antibacterial and bioimaging applications. Sci Rep. 2023;13(1):9676.
[50] Wang YK. Preparation, properties and application of carbon dots based on two fruits of peels [dissertation]. Shaanxi, China: Xi'an University of Science and Technology; 2022. Chinese.
[51] Qi H, Teng M, Liu M, Liu S, Li J, Yu H, et al. Biomass-derived nitrogen-doped carbon quantum dots: highly selective fluorescent probe for detecting Fe3+ ions and tetracyclines. J Colloid Interface Sci. 2019;539:332–41.
[52] Yuan M, Zhong R, Gao H, Li W, Yun X, Liu J, et al. One-step, green, and economic synthesis of water-soluble photoluminescent carbon dots by hydrothermal treatment of wheat straw, and their bio-applications in labeling, imaging, and sensing. Appl Surf Sci. 2015;355:1136–44.
[53] Wu Y, Li Y, Pan X, Hu C, Zhuang J, Zhang X, et al. Hemicellulose-triggered high-yield synthesis of carbon dots from biomass. New J Chem. 2021;45(12):5484–90.
[54] Xu Y, Lan J, Wang B, Bo C, Ou J, Gong B. Simple fabrication of carbon quantum dots and activated carbon from waste wolfberry stems for detection and adsorption of copper ion. RSC Adv. 2023;13(31):21199–210.
[55] Man Y, Li Z, Kong WL, Li W, Dong W, Wang Y, et al. Starch fermentation wastewater as a precursor to prepare S, N-doped carbon dots for selective Fe (III) detection and carbon microspheres for solution decolorization. Microchem J. 2020;159:105338.
[56] Setianto S, Men LK, Bahtiar A, Panatarani C, Joni IM. Carbon quantum dots with honeycomb structure: a novel synthesis approach utilizing cigarette smoke precursors. Sci Rep. 2024;14(1):1996.
[57] Korram J, Koyande P, Mehetre S, Sawant SN. Biomass-derived carbon dots as nanoprobes for smartphone–paper-based assay of iron and bioimaging application. ACS Omega. 2023;8(34):31410–8.
[58] Li SP. Preparation and photocatalytic properties of wood-based carbon quantum dots/zinc oxide composites [dissertation]. Heilongjiang, China: Northeast Forestry University; 2022. Chinese.
[59] Fu Y, Xu H, Guo Q, Yang D, Pan Y, Xue Z. Preparation of wood-based carbon quantum dots and promotion of light capture applications. Coatings. 2024;14(4):417.
[60] Sandeep DH, Krushna BR, Sharma SC, Ravindran P, Sivayogana R, Ramesha H, et al. Eco-friendly synthesis of CQDs from Pistachio shells: Versatile applications in anti-counterfeiting, flexible films, latent fingerprints and potential anti-cancer activity. J Alloys Compd. 2024;991:174311.
[61] Liu Q, Li W, Qiao X, Zhao H. Composition analysis of Magnolia flower and their use for highly bright carbon dots. Ind Crops Prod. 2024;213:118416.
[62] Krushna BR, Sandeep DH, Manjunatha K, Sharma SC, Panda M, Krithika C, et al. Sustainable latent fingerprint enhancement with ink-free printing and shape memory behavior using Parthenium Hysterophorus-derived carbon dots. SM&T. 2024;40:e00951.
[63] John BK, Mathew J, Sreekanth K, Mathew B. Biomass derived carbon quantum dots as a versatile platform for fluorescent sensing, catalytic reduction, fluorescent ink and anticancer agents. Mater Today Sustain. 2024;26:100715.
[64] Long X, Wang J, Ma Y, Wu S. Synthesis of high-performance carbon dots from laurel leaves and their application in anti-counterfeit ink. Colloids Surf A Physicochem Eng Asp. 2023;676:132136.
[65] Atchudan R, Kishore SC, Gangadaran P, Edison TN, Perumal S, Rajendran RL, et al. Tunable fluorescent carbon dots from biowaste as fluorescence ink and imaging human normal and cancer cells. Environ Res. 2022;204:112365.
[66] Hong WT, Yang HK. Anti-counterfeiting application of fluorescent carbon dots derived from wasted coffee grounds. Optik. 2021;241:166449.

[67] Gong X, Gao X, Du W, Zhang H, Zhang S, Nguyen TT, et al. Wood powder-derived quantum dots for CeO_2 photocatalytic and anti-counterfeit applications. Opt Mater. 2019;96:109302.
[68] Huang K, He Q, Sun R, Fang L, Song H, Li L, et al. Preparation and application of carbon dots derived from cherry blossom flowers. Chem Phys Lett. 2019;731:136586.
[69] Liang Z, Zeng L, Cao X, Wang Q, Wang X, Sun R. Sustainable carbon quantum dots from forestry and agricultural biomass with amplified photoluminescence by simple NH_4OH passivation. J Mater Chem C. 2014;2(45):9760–6.
[70] Rodríguez-Carballo G, García-Sancho C, Algarra M, Castro E, Moreno-Tost R. One-pot synthesis of green-emitting nitrogen-doped carbon dots from xylose. Catalysts. 2023;13(10):1358.
[71] Su H, Bi Z, Ni Y, Yan L. One-pot degradation of cellulose into carbon dots and organic acids in its homogeneous aqueous solution. Green Energy Environ. 2019;4(4):391–9.
[72] Liu Z, Chen M, Guo Y, Zhou J, Shi Q, Sun R. Oxidized nanocellulose facilitates preparing photoluminescent nitrogen-doped fluorescent carbon dots for Fe^{3+} ions detection and bioimaging. Chem Eng J. 2020;384:123260.
[73] Yang X, Guo Y, Liang S, Hou S, Chu T, Ma J, et al. Preparation of sulfur-doped carbon quantum dots from lignin as a sensor to detect Sudan I in an acidic environment. J Mater Chem B. 2020;8(47):10788–96.
[74] Yang X, Hou S, Chu T, Han J, Li R, Guo Y, et al. Preparation of magnesium, nitrogen-codoped carbon quantum dots from lignin with bright green fluorescence and sensitive pH response. Ind Crops Prod. 2021;167:113507.
[75] Zhu L, Shen D, Wang Q, Luo KH. Green synthesis of tunable fluorescent carbon quantum dots from lignin and their application in anti-counterfeit printing. ACS Appl Mater Interfaces. 2021;13(47):56465–75.
[76] Sebei K, Sakouhi F, Herchi W, Khouja ML, Boukhchina S. Chemical composition and antibacterial activities of seven Eucalyptus species essential oils leaves. Biol Res. 2015;48:1–5.
[77] Klongklaw K, Phiromkaew B, Kiatsuksri P, Kankit B, Anantachaisilp S, Wechakorn K. Green one-step synthesis of mushroom-derived carbon dots as fluorescent sensors for Fe^{3+} detection. RSC Adv. 2023;13(44):30869–75.
[78] Mu M, Duan Z, Fan S, Zhao W, Gao W, Bai R, et al. Detection of ferric ions by nitrogen and sulfur co-doped potato-derived carbon quantum dots as a fluorescent probe. Mater Res Express. 2024;11(4):045501.
[79] Zhang YQ. Preparation and application of carbon quantum dots from authentic medicinal materials in Shanxi [dissertation]. Shanxi, China: Shanxi University; 2021. Chinese.
[80] Miao H, Wang Y, Yang X. Carbon dots derived from tobacco for visually distinguishing and detecting three kinds of tetracyclines. Nanoscale. 2018;10(17):8139–45.
[81] Cao X. Green synthesis and analytical application of fluorescent carbon quantum dots [dissertation]. Anhui, China: Huaibei Normal University; 2022. Chinese.
[82] Cui Y, Liu R, Ye F, Zhao S. Single-excitation, dual-emission biomass quantum dots: preparation and application for ratiometric fluorescence imaging of coenzyme A in living cells. Nanoscale. 2019;11(19):9270–5.
[83] Xie Y, Cheng D, Liu X, Han A. Green hydrothermal synthesis of N-doped carbon dots from biomass highland barley for the detection of Hg^{2+}. Sensors. 2019;19(14):3169.
[84] Xu Y, Fan Y, Zhang L, Wang Q, Fu H, She Y. A novel enhanced fluorescence method based on multifunctional carbon dots for specific detection of Hg^{2+} in complex samples. Spectrochim Acta A Mol Biomol Spectrosc. 2019;220:117109.
[85] Zulfajri M, Sudewi S, Damayanti R, Huang GG. Rambutan seed waste-derived nitrogen-doped carbon dots with l-aspartic acid for the sensing of Congo red dye. RSC Adv. 2023;13(10):6422–32.
[86] Li Z, Zhang Y, Niu Q, Mou M, Wu Y, Liu X, et al. A fluorescence probe based on the nitrogen-doped carbon dots prepared from orange juice for detecting Hg^{2+} in water. J Lumin. 2017;187:274–80.
[87] Atchudan R, Edison TN, Aseer KR, Perumal S, Karthik N, Lee YR. Highly fluorescent nitrogen-doped carbon dots derived from Phyllanthus acidus utilized as a fluorescent probe for label-free selective detection of Fe3 + ions, live cell imaging and fluorescent ink. Biosens Bioelectron. 2018;99:303–11.
[88] Hidayat RN, Widiyandari H, Parasdila H, Prilita O, Astuti Y, Mufti N, et al. Green synthesis of ZnO photocatalyst composited carbon quantum dots (CQDs) from lime (Citrus aurantifolia). Catal Commun. 2024;187:106888.
[89] Atchudan R, Edison TN, Lee YR. Nitrogen-doped carbon dots originating from unripe peach for fluorescent bioimaging and electrocatalytic oxygen reduction reaction. J Colloid Interface Sci. 2016;482:8–18.
[90] Wang N, Wang Y, Guo T, Yang T, Chen M, Wang J. Green preparation of carbon dots with papaya as carbon source for effective fluorescent sensing of Iron (III) and Escherichia coli. Biosens Bioelectron. 2016;85:68–75.
[91] Bhamore JR, Jha S, Singhal RK, Park TJ, Kailasa SK. Facile green synthesis of carbon dots from Pyrus pyrifolia fruit for assaying of Al^{3+} ion via chelation enhanced fluorescence mechanism. J Mol Liq. 2018;264:9–16.
[92] Zhang Q, Wang X, Yuan L, Yu L, Shao C, Jia H, et al. Nitrogen-doped biomass-derived carbon dots for fluorescence determination of sunset yellow. Anal Methods. 2024;16(14):2063–70.
[93] Atchudan R, Edison TN, Chakradhar D, Perumal S, Shim JJ, Lee YR. Facile green synthesis of nitrogen-doped carbon dots using Chionanthus retusus fruit extract and investigation of their suitability for metal ion sensing and biological applications. Sens Actuators B Chem. 2017;246:497–509.
[94] Senol AM, Bozkurt E. Facile green and one-pot synthesis of seville orange derived carbon dots as a fluorescent sensor for Fe^{3+} ions. Microchem J. 2020;159:105357.
[95] Wang L, Zheng S, Liu Y, Ji Y, Liu X, Wang F, et al. A nanozyme multifunctional platform based on iron doped carbon dots derived from Tibetan Ganoderma lucidum waste for glucose sensing, anti-counterfeiting applications, and anticancer cell effect. Talanta. 2024;276:126262.
[96] Alam MW. Hydrothermally synthesized fluorescent nitrogen-doped carbon dots for catalytic efficiency and anti-counterfeiting application. Opt Mater. 2024;152:115401.
[97] Ma H, Guan L, Chen M, Zhang Y, Wu Y, Liu Z, et al. Synthesis and enhancement of carbon quantum dots from Mopan persimmons for Fe3+ sensing and anti-counterfeiting applications. Chem Eng J. 2023;453:139906.
[98] Zhang L, Luo W, Chen Y, Zheng J, Cao L, Duan L, et al. Green synthesis of boron-doped carbon dots from Chinese herbal residues for Fe3+ sensing, anti-counterfeiting, and photodegradation applications. J Clean Prod. 2023;422:138577.

[99] Liao S, Long X, Ma Y, Wu S, Wang J. Synthesis of multicolor fluorescent carbon dots from zanthoxylum bungeanum and their application in fluorescent anti-counterfeiting ink. J Photochem Photobiol A. 2023;445:115066.
[100] Wang J, Sun Y, Wang P, Sun Z, Wang Y, Gao M, et al. A dual-emitting fluoroprobe fabricated by aloe leaf-based N-doped carbon quantum dots and copper nanoclusters for nitenpyram detection in waters by virtue of inner filter effect and static quenching principles. Anal Chim Acta. 2024;1289:342182.
[101] Ullal N, Lewis PM, Sunil D, Kulkarni SD, Anand PJ, Bhat U. Dual emissive water-based flexo ink from tapioca-derived carbon dots for anti-counterfeiting applications. Prog Org Coat. 2022;173:107233.
[102] Hong WT, Yang HK. Luminescent properties of carbon dots originated from pine pollen for anti-counterfeiting application. Opt Laser Technol. 2022;145:107452.
[103] Xavier SS, Siva G, Annaraj J, Kim AR, Yoo DJ. Sensitive and selective turn-off-on fluorescence detection of Hg^{2+} and cysteine using nitrogen doped carbon nanodots derived from citron and urine. Sens Actuators B Chem. 2018;259:1133–43.
[104] Yao L, Zhao MM, Luo QW, Zhang YC, Liu TT, Yang Z, et al. Carbon quantum dots-based nanozyme from coffee induces cancer cell ferroptosis to activate antitumor immunity. ACS Nano. 2022;16(6):9228–39.
[105] Tang X, Yang X, Yu Y, Wu M, Li Y, Zhang Z, et al. Carbon quantum dots of ginsenoside Rb1 for application in a mouse model of intracerebral Hemorrhage. J Nanobiotechnol. 2024;22(1):125.
[106] Zhou C. Preparation and application of carbon quantum dots from biomass as a carbon source [dissertation]. Qinghai, China: Qinghai University; 2022. Chinese.
[107] Guo B, Chen F, Liu G, Li W, Li W, Zhuang J, et al. Effects and mechanisms of proanthocyanidins-derived carbon dots on alleviating salt stress in rice by muti-omics analysis. Food Chem X. 2024;22:101422.
[108] Serag E, Helal M, El Nemr A. Curcumin loaded onto folic acid carbon dots as a potent drug delivery system for antibacterial and anticancer applications. J Clust Sci. 2024;35(2):519–32.
[109] Smrithi SP, Kottam N, Vergis BR. Heteroatom modified hybrid carbon quantum dots derived from Cucurbita pepo for the visible light driven photocatalytic dye degradation. Top Catal. 2022;68:1427–38.
[110] Zhang Y, Gao Z, Yang X, Chang J, Liu Z, Jiang K. Fish-scale-derived carbon dots as efficient fluorescent nanoprobes for detection of ferric ions. RSC Adv. 2019;9(2):940–9.
[111] Hastuti E, Salsadilla C, Sari AY, Hikmah U. The hydrothermal effect of time and temperature on the synthesis of carbon dots from chicken feathers. IOP Conf Ser Earth Environ Sci. 2024;1312(1):012018.
[112] Chen J, Xia X, Li P, Yu H, Xie Y, Guo Y, et al. Crayfish shells-derived carbon dots as a fluorescence sensor for the selective detection of 4-nitrophenol. Food Agric Immunol. 2023;34(1):36–47.
[113] Shen Y, Zhang R, Wang Y. One-pot hydrothermal synthesis of metal-doped carbon dot nanozymes using protein cages as precursors. RSC Adv. 2023;13(10):6760–7.
[114] Ni Y, Zhou P, Jiang Q, Zhang Q, Huang X, Jing Y. Room-temperature phosphorescence based on chitosan carbon dots for trace water detection in organic solvents and anti-counterfeiting application. Dyes Pigments. 2022;197:109923.
[115] Başkaya SK, Tahta B, Uruş S, Eskalen H, Çeşme M, Özğan Ş. Multifunctional B, N, P, and S-doped fluorescent carbon quantum dot synthesis from pigeon manure: highly effective Hg(II) sensor and fluorescent ink properties. Biomass Convers Biorefin. 2024;14(1):1089–103.
[116] Song Y, Qi N, Li K, Cheng D, Wang D, Li Y. Green fluorescent nanomaterials for rapid detection of chromium and iron ions: wool keratin-based carbon quantum dots. RSC Adv. 2022;12(13):8108–18.
[117] Kumar A, Kumar I, Gathania AK. Synthesis, characterization and potential sensing application of carbon dots synthesized via the hydrothermal treatment of cow milk. Sci Rep. 2022;12(1):22495.
[118] Han S, Zhang H, Xie Y, Liu L, Shan C, Li X, et al. Application of cow milk-derived carbon dots/Ag NPs composite as the antibacterial agent. Appl Surf Sci. 2015;328:368–73.
[119] Ye H, Liu B, Wang J, Zhou C, Xiong Z, Zhao L. A hydrothermal method to generate carbon quantum dots from waste bones and their detection of laundry powder. Molecules. 2022;27(19):6479.
[120] Zhao W, Zhang Y, Cao B, Li Z, Sun C, Cao X, et al. Characteristics of mussels-derived carbon dots and their applications in bio-imaging and detection of riboflavin. Foods. 2022;11(16):2451.
[121] Elango D, Packialakshmi JS, Manikandan V, Jayanthi P. Synthesis of crab-shell derived CQDs for Cd^{2+} detection and antibacterial applications. Mater Lett. 2022;313:131822.
[122] Wu L, Pan W, Ye H, Liang N, Zhao L. Sensitive fluorescence detection for hydrogen peroxide and glucose using biomass carbon dots: dual-quenching mechanism insight. Colloids Surf A Physicochem Eng Asp. 2022;638:128330.
[123] Tai JY, Leong KH, Saravanan P, Tan ST, Chong WC, Sim LC. Facile green synthesis of fingernails derived carbon quantum dots for Cu^{2+} sensing and photodegradation of 2,4-dichlorophenol. J Environ Chem Eng. 2021;9(1):104622.
[124] Narimani S, Samadi N. Rapid trace analysis of ceftriaxone using new fluorescent carbon dots as a highly sensitive turn-off nanoprobe. Microchem J. 2021;168:106372.
[125] Chen W, Fan J, Wu X, Hu D, Wu Y, Feng Z, et al. Facile synthesis of nitrogen-doped carbon dots from pork liver and its sensing of 6-thioguanine based on the inner filter effect. New J Chem. 2021;45(11):5114–20.
[126] Surendran P, Lakshmanan A, Priya SS, Balakrishnan K, Rameshkumar P, Kannan K, et al. Bioinspired fluorescence carbon quantum dots extracted from natural honey: efficient material for photonic and antibacterial applications. Nano-Struct Nano-Objects. 2020;24:100589.
[127] Wang Q, Cai J, Biesold-McGee GV, Huang J, Ng YH, Sun H, et al. Silk fibroin-derived nitrogen-doped carbon quantum dots anchored on TiO_2 nanotube arrays for heterogeneous photocatalytic degradation and water splitting. Nano Energy. 2020;78:105313.
[128] Sahoo NK, Das S, Jana GC, Aktara MN, Patra A, Maji A, et al. Eco-friendly synthesis of a highly fluorescent carbon dots from spider silk and its application towards Hg(II) ions detection in real sample and living cells. Microchem J. 2019;144:479–88.
[129] Dehghani A, Ardekani SM, Hassan M, Gomes VG. Collagen derived carbon quantum dots for cell imaging in 3D scaffolds via two-photon spectroscopy. Carbon. 2018;131:238–45.
[130] Zhang Y, Gao Z, Zhang W, Wang W, Chang J, Kai J. Fluorescent carbon dots as nanoprobe for determination of lidocaine hydrochloride. Sens Actuators B Chem. 2018;262:928–37.
[131] Zhao C, Jiao Y, Hu F, Yang Y. Green synthesis of carbon dots from pork and application as nanosensors for uric acid detection. Spectrochim Acta A Mol Biomol Spectrosc. 2018;190:360–7.

[132] Liu H, Zhang Y, Liu JH, Hou P, Zhou J, Huang CZ. Preparation of nitrogen-doped carbon dots with high quantum yield from Bombyx mori silk for Fe(III) ions detection. RSC Adv. 2017;7(80):50584–90.
[133] Wang S, Niu H, He S, Cai Y. One-step fabrication of high quantum yield sulfur- and nitrogen-doped carbon dots for sensitive and selective detection of Cr(VI). RSC Adv. 2016;6(109):107717–22.
[134] Wen X, Shi L, Wen G, Li Y, Dong C, Yang J, et al. Green and facile synthesis of nitrogen-doped carbon nanodots for multicolor cellular imaging and Co^{2+} sensing in living cells. Sens Actuators B Chem. 2016;235:179–87.
[135] Zhang H, Kang S, Wang G, Zhang Y, Zhao H. Fluorescence determination of nitrite in water using prawn-shell derived nitrogen-doped carbon nanodots as fluorophores. ACS Sens. 2016;1(7):875–81.
[136] He J, Lei B, Zhang H, Zheng M, Dong H, Zhuang J, et al. Using hydrogen peroxide to mediate through a one-step hydrothermal method for the fast and green synthesis of N-CDs. RSC Adv. 2015;5(116):95744–9.
[137] Mirseyed PS, Arjmand S, Rahmandoust M, Kheirabadi S, Anbarteh R. Green synthesis of yeast cell wall-derived carbon quantum dots with multiple biological activities. Heliyon. 2024;10(9):e20953.
[138] Zhang L, Wang Y, Jia L, Zhang X, Xu J. Dynamic anti-counterfeiting and reversible multi-level encryption-decryption based on spirulina derived pH-responsive dual-emissive carbon dots. J Lumin. 2023;257:119727.
[139] Hu J, Zhou H, Ma Y, Wu S, Hao L. Green synthesis of carbon dots from cordyceps militaris and versatile applications in alcohol detection and waterproof fluorescent ink. Opt Mater. 2023;142:114057.
[140] Shen J, He Z, Zhang J, Guo H, Lin W, Gu H. Green and sustainable preparation of functionalized carbon quantum dots and fluorescent hydrogel from exopolysaccharides for multiple fluorescence applications. Polymer. 2023;288:126471.
[141] Kalpana R, Vignesh NS, Vinothini K, Rajan M, Ashokkumar B, Brindhadevi K, et al. Carbon quantum dots (CQD) fabricated from Exiguobacterium sp. VK2 exopolysaccharide (EPS) using hydrothermal reaction and its biodiesel applications. Fuel. 2023;333:126426.
[142] Liu Y, Zhou L, Li Y, Deng R, Zhang H. Highly fluorescent nitrogen-doped carbon dots with excellent thermal and photo stability applied as invisible ink for loading important information and anti-counterfeiting. Nanoscale. 2017;9(2):491–6.
[143] Oklevski S. Poroscopy: qualitative and quantitative analysis of the 2nd and 3rd level detail and their relation. Fingerprint Whorld. 2011;37(145):170–81.
[144] Narasimhamurthy KN, Krushna BR, Manjunatha K, Chiu HH, Subramanian B, Wu SY, et al. Novel intense blue emitting $Bi_2Zr_2O_7:Ce^{3+}$ nanocomposites insertion into flexible polymer films for anti-counterfeiting, long-term storage fingerprints, and display device applications. Mater Today Commun. 2023;37:106883.
[145] Krushna BR, Sharma SC, Prasad BD, Sridhar C, Varalakshmi S, George A, et al. A new strategy to boost luminescent markers for LFP detection and anti-counterfeiting applications using flux assisted $BaLa_2ZnO_5:Eu^{3+}$ phosphor. Mater Res Bull. 2024;170:112561.
[146] Sun Y, Le X, Zhou S, Chen T. Recent progress in smart polymeric gel-based information storage for anti-counterfeiting. Adv Mater. 2022;34(41):2201262.
[147] Liu Y, Meng L, Wang H, Jiao J, Xing M, Peng Y, et al. Promising lanthanide-doped BiVO4 phosphors for highly efficient upconversion luminescence and temperature sensing. Dalton Trans. 2021;50(3):960–9.
[148] Shen J, Xu Y, Wang Z, Chen W, Zhao H, Liu X. Facile and green synthesis of carbon nanodots from environmental pollutants for cell imaging and Fe^{3+} detection. New J Chem. 2022;46(26):12581–8.
[149] Chen W, Shen J, Wang Z, Liu X, Xu Y, Zhao H, et al. Turning waste into wealth: facile and green synthesis of carbon nanodots from pollutants and applications to bioimaging. Chem Sci. 2021;12(35):11722–9.
[150] Muthamma K, Sunil D, Shetty P. Luminophoric organic molecules for anticounterfeit printing ink applications: an up-to-date review. Mater Today Chem. 2020;18:100361.
[151] Tripti T, Singh P, Rani N, Kumar S, Kumar K, Kumar P. Carbon dots as potential candidate for photocatalytic treatment of dye wastewater. Environ Sci Pollut Res. 2024;31(5):6738–65.
[152] Liu X, Wang Y, Gu Y, Lu W. One-step hydrothermal synthesis of nitrogen-doped carbon-quantum-dots for detection and efficient removal of high-concentrations nicotine from tobacco wastewater under visible light. Chem Eng J. 2024;499:156573.
[153] Sabet M, Mahdavi K. Green synthesis of high photoluminescence nitrogen-doped carbon quantum dots from grass via a simple hydrothermal method for removing organic and inorganic water pollutions. Appl Surf Sci. 2019;463:283–91.
[154] Singh P, Kumar S, Kumar P, Kataria N, Bhankar V, Kumar K, et al. Assessment of biomass-derived carbon dots as highly sensitive and selective templates for the sensing of hazardous ions. Nanoscale. 2023;15(40):16241–67.
[155] Shekarbeygi Z, Farhadian N, Khani S, Moradi S, Shahlaei M. The effects of rose pigments extracted by different methods on the optical properties of carbon quantum dots and its efficacy in the determination of Diazinon. Microchem J. 2020;158:105232.
[156] Wang QY, Xu YX, Cai ZX, Chen YP, Huang X, Ma MH, et al. Progress in the preparation and application of food-derived carbon dots. Food Sci. 2020;41(9):301–9. Chinese.
[157] Barus DA, Ginting AR, Ginting J, Ginting RT, Pepayosa BE. Synthesis of carbon dots from butterfly pea (Clitoria ternatea) as detection of the heavy metal ion Cu^{2+}. J Phys Conf Ser. 2024;2733(1):012005.
[158] Radnia F, Mohajeri N, Zarghami N. New insight into the engineering of green carbon dots: possible applications in emerging cancer theranostics. Talanta. 2020;209:120547.
[159] Singh P, Bhankar V, Kumar S, Kumar K. Biomass-derived carbon dots as significant biological tools in the medicinal field: a review. Adv Colloid Interface Sci. 2024;328:103182.
[160] Tejwan N, Saha SK, Das J Multifaceted applications of green carbon dots synthesized from renewable sources. Adv Colloid Interface Sci. 2020;275:102046.